UNIVERSIDAD
NACIONAL
DE COLOMBIA

Chaos and randomness in a classical bistable system coupled to a finite heat bath

Santiago Peña Martínez

Universidad Nacional de Colombia

This dissertation is submitted on July, 2020 for the degree of Bachelor in Physics

Declaration

This dissertation is the result of my own work and includes nothing which is the outcome of work done in collaboration except as declared in the Preface and specified in the text. It is not substantially the same as any that I have submitted, or am concurrently submitting, for a degree or diploma or other qualification at the Universidad Nacional de Colombia or any other University or similar institution except as declared in the Preface and specified in the text. I further state that no substantial part of my dissertation has already been submitted, or is being concurrently submitted, for any such degree, diploma or other qualification at the Universidad Nacional de Colombia or any other University or similar institution except as declared in the Preface and specified in the text.

Santiago Peña Martínez
Month, Year

Abstract

Chaos and randomness in a classical bistable system coupled to a finite heat bath

Santiago Peña Martínez

In this work we study a double well potential coupled to a finite heat bath consisting of N harmonic oscillators. For $N = 1$, the system will oscillate in an iregular manner between the symmetric minima involving chaotic properties. As we increase N to values > 1, the system will approach a bistable behaviour, according to the microscopic theory of dissipation. In particular, the system will irreversibly fall into one of the wells, imitating the result of a measurement of two alternative states. Which well it chooses will depend on the initial state of the system and the heat bath, meaning that the information encoded in the microscopic initial conditions is amplified and recorded in the final state, as in a measurement.

Keywords: Chaos, Dissipation, Measurement.

Acknowledgements

My acknowledgements ...

Contents

CHAPTER 1

Introduction

The concept of measurement in quantum mechanics has been a fuzzy concept ever since the origins of the quantum theory because there is not a precise description of what happens when physicists say that the wave function "collapses". This lack of description about the moment of the collapse and the inability to observe this phenomenom directly lead to different interpretations of quantum mechanics [1]. In this work we do not intent to solve this problem in the quantum mechanics frame but we will show an approach to study this problem by looking at a classical analogue of the spin and describing in classical terms the effect that an environment has in the outcome of what we will call a measurement.

When considering the effects of an environment enclosing a system of interest, most of the times you arrive to a problem that is difficult model and solve. Generally when trying to model an environment it consists of a large number of degrees of freedom, this leads to adopting tools such as Langevin dynamics and statistical methods to try to solve this problem, this makes microscopic effects on the system have a role in the macroscopic dynamics.

Some of the first approaches to model environments in statistical physics where made to model properly the Browinian motion [2][3][4]. The original Langevin equation [5] was used to describe Brownian motion, this approach consists on describing the system in a way that all of the effects of the environment are contained in a time-dependent force term and a velocity dependent friction of damping term. The force term behaves as a stochastic process representing the "randomness" of the environment affecting the central system. This method is widely used to study the properties of the central system without going into the details of the environment. It is important to state here that the environment is and will be considered as a heat bath in the thermodynamic sense, where the central system can exchange energy back and forth in time until thermal equilibrium is reached.

The study of open systems is a very active branch in quantum and classical mechanics, most of these studies involve the use of numerical schemes to solve differential equations that may not be integrable analytically by modeling the heat bath as an ensemble of harmonic oscillators [6][7][8]. Langevin dynamics on these types of model in the case of infinite number of linear harmonic oscillators in the heat bath lead to irreversible energy flow from the test particle into the bath and therefore achieves thermalization when the test particle posses a Boltzmann distribution. Several of the studies made before regarding modeling of open systems as finite heat baths coupled to a test particle also managed thermalization of the test particle [6][9][10][11]. This type of modeling is closely related to the one used in dissipation involved in quantum mechanics where the system of interest is coupled to a set of non interacting harmonic oscillators that posses a continuous linear frequency distribution known as the Caldeira-Leggett model [12].

In this work we will use the model described by Leggett et al. [13] for dissipative two state quantum systems and treat it as a classical problem described as a double well potential, this system we will couple it to a finite heat bath and study its dynamics by steadily increasing the number of harmonic oscillators in the heat bath. This type of modeling will give some insight about a classical analogue of the quantum spin measurement and will help to describe some of the effects that the environment (in this case the heat bath) will have in the result of the final dynamics of a dissipative system that can be considered as a classical measurement analogue of the quantum one. We will show the analytical properties of the particle in the double well potential and how it is a chaotic system when started initially in the unstable equilibrium point. Using numerical symplectic algorithms we will solve the equations of motions for different numbers of harmonic oscillators in the heat bath until we achieve the behavior expected of dissipative dynamics of an infinite heat bath but using a finite number of modes.

We can mimic randomness of the quantum measurement in this system by using the chaotical properties of this classical scenario. As the unstable equilibrium point is chaotic as its dynamics evolves in time, when we couple this central system to a finite heat bath on an initial "neutral" state, due to the heat bath not being perfectly symmetric the particle in the central system will amplify this asymmetries and will lead to the particle falling on different sides of the double well potential. In this picture we can compare it to a certain degree to what happens on a measurement of a two state quantum system, say the spin measurement of the Stern-Gerlach experiment.

CHAPTER 2

Hamiltonian systems and Symplectic structure

In this chapter we are going to introduce some important concepts regarding dynamical systems and how they relate to hamiltonian systems and its geometric structure. Also we describe the theory involving the numerical integration of differential equations conserving the symplectic structure. These descriptions are made mostly following Ref. [14] and Ref. [15].

2.1 Dynamical systems

Generally speaking, a dynamical system may be defined as set of deterministic mathematical equations whose solution shows how the system evolves in time. Time may be taken as a continuous or a discrete variable. A typical example of a dynamical system that adopts time as a parameter varying in a continuous way is a system of n first order, autonomous, ordinary differential equations,

$$\begin{aligned} \frac{dx^{(1)}}{dt} &= F_1(x^{(1)}, x^{(2)}, ..., x^{(n)}), \\ \frac{dx^{(2)}}{dt} &= F_2(x^{(1)}, x^{(2)}, ..., x^{(n)}), \\ &\vdots \\ \frac{dx^{(n)}}{dt} &= F_n(x^{(1)}, x^{(2)}, ..., x^{(n)}), \end{aligned} \tag{2.1}$$

we can rewrite this set of equations by adopting a notation for a compact equation using the vector form of equations

$$\frac{d\vec{x}(t)}{dt} = \vec{F}[\vec{x}(t)], \tag{2.2}$$

here we take $\vec{x}$ as an n dimensional vector that represents the state of the system at a given time t and $\vec{F}$ is a function depending on the variable $\vec{x}$. This set of equations represent a dynamical system, for an initial state given by $\vec{x}(0)$, it is possible in principle to be able to solve this set of equations in time and retrieve the state $\vec{x}(t)$ of the system for any given $t > 0$. The figure (2.1) shows the points followed as the system evolves in time for the case of $n = 3$. The space $(x^{(1)}, x^{(2)}x^{(3)}$ in the figure is more known as the phase space, and the path in the phase space is referred as orbit or trajectory. When we speak of dynamical systems using continuous time, it is common to refer to these orbits as a flow.

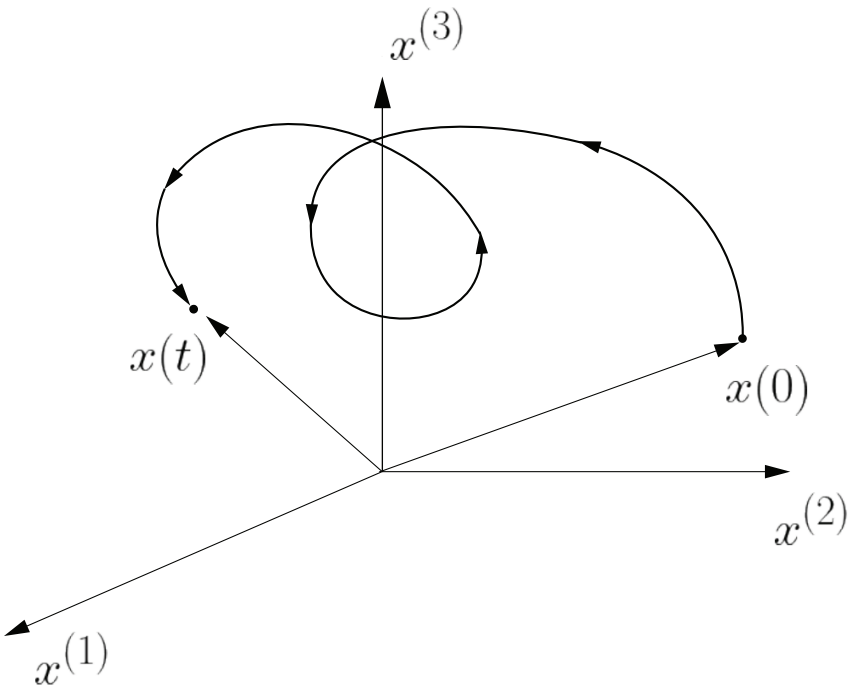

Figure 2.1: Orbit in three dimensional phase space

For the case of discrete systems, time is represented as integer values ($t = 1, 2, 3, ...$). The

best example of a dynamical system with discrete time is a map, which can be written in vector notation as

$_{t+1} = \vec{M}(\vec{x}_t)$(2.3)where $\vec{x}_t$ is an n-dimensional vector $\vec{x}_t = (x_t^1, x_t^2, ..., x_t^n)$ and $\vec{M}$ a function of $\vec{x}_t$. Given an initial state $\vec{x}_0$, it is possible to obtain the state at time $t = 1$ by applying the map $\vec{x}_1 = \vec{M}(\vec{x}_0)$. Having determined $\vec{x}_1$ it will be possible to determine the state at time $t = 2$ by applying the map again but to the new state at $t = 1$ as $\vec{x}_2 = \vec{M}(\vec{x}_1)$ and so on. Thus, given an initial condition $\vec{x}_0$ we generate a trajectory of the discrete time system in time: $\vec{x}_0, \vec{x}_1, \vec{x}_2, ...$

A dynamical system that posses continuous time evolution may be reduced to a discrete time system to evaluate in more detail the dynamical properties of the system, this is done by using the technique called Poincaré Surface Section. To do so we consider a set of n first order, autonomous, ordinary differential equations such as in (2.2), a Poincaré map represents a reduction of the flow in the n-dimensional space to a map of dimension $n - 1$. To illustrate this, an example with $n = 3$ is given:

FIGURA
QUE
NO
HE
HECHO

Fig (NUMERO DE LA FIGURA) shows a Poincaré section on a two dimensional plane S where the fixed condition will be $x^3 = constant$. The points labeled as A and B represent the succesive intersections of the trajectory followed by the system with the plane S, this crossing is always considered to be on the same direction, a crossing of the plane through the opposite direction will result into another section. Given the point A, by using Equation (2.2), we can certainly determine the position of point B, this is because A can be used as an initial condition to determine B. The same argument can be used to determine A given B as initial condition, this is done just by changing the sign of time on the same equation. Thus, the Poincaré map in this illustration represents an invertible two dimensional map that transforms the coordinates $(x_n^{(1)}, x_n^{(2)})$ of the nth piercing of the surface section to the coordinates $(x_{n+1}^{(1)}, x_{n+1}^{(2)})$ at piercing $n+1$. This map can be generalized to an N dimensional flow with an $N - 1$ dimensional invertible map.

2.2 Hamilton equations and Symplectic Structure

Hamiltonian systems are a class of dynamical systems that occur in a wide variety of circumstances, the special properties of Hamilton's equations of motion that are characteristic of this kind of systems endow Hamiltonian systems with attributes that differ qualitatively and fundamentally from other systems.

The dynamics of a Hamiltonian system can be completely determined by a single function commonly known as the Hamiltonian, $H(\boldsymbol{p}, \boldsymbol{q}, t)$. The state of the system is specified by its "momentum" and "position" usually known as $\boldsymbol{p}$ and $\boldsymbol{q}$ respectively, both vectors with dimension N. N is also known as the number of degrees of freedom of the system. Given the Hamilton's equations, the we can determine the trajectory $(\boldsymbol{p}(t), \boldsymbol{q}(t))$ that the system follows in the $2N$ dimensional phase space, these equations are given by

$$\frac{d\boldsymbol{p}}{dt} = -\frac{\partial H(\boldsymbol{p}, \boldsymbol{q}, t)}{\partial \boldsymbol{q}}, \tag{2.4}$$

$$\frac{d\boldsymbol{q}}{dt} = \frac{\partial H(\boldsymbol{p}, \boldsymbol{q}, t)}{\partial \boldsymbol{p}}. \tag{2.5}$$

In the special case where the Hamiltonian has no explicit time dependance, $H = H(\boldsymbol{p}, \boldsymbol{q})$, given Hamilton's equations of motion it can be deduced that as $\boldsymbol{p}$ and $\boldsymbol{q}$ vary with time, the value of $H(\boldsymbol{p}(t), \boldsymbol{q}(t))$ remains constant:

$$\frac{dH}{dt} = \frac{d\boldsymbol{q}}{dt}\frac{\partial H(\boldsymbol{p}, \boldsymbol{q})}{d\boldsymbol{q}} + \frac{d\boldsymbol{p}}{dt}\frac{\partial H(\boldsymbol{p}, \boldsymbol{q})}{d\boldsymbol{p}} = \frac{\partial H(\boldsymbol{p}, \boldsymbol{q})}{d\boldsymbol{p}}\frac{\partial H(\boldsymbol{p}, \boldsymbol{q})}{d\boldsymbol{q}} - \frac{\partial H(\boldsymbol{p}, \boldsymbol{q})}{d\boldsymbol{q}}\frac{\partial H(\boldsymbol{p}, \boldsymbol{q})}{d\boldsymbol{p}} = 0$$

Thus if we identify the value of the Hamiltonian as the energy E of the system, we conclude that the energy is conserved in the case of time independent systems, $E = H(\boldsymbol{p}, \boldsymbol{q}) = constant$ [14].

Another interesting feature of Hamilton equations and Hamiltonian systems is that we can write Equations (2.4, 2.5) in matrix form as

$$\frac{d\tilde{\boldsymbol{x}}}{dt} = \boldsymbol{F}(\tilde{\boldsymbol{x}}, t), \tag{2.6}$$

by taking $\tilde{\boldsymbol{x}}$ to be the $2N$ dimensional vector

$$\tilde{\boldsymbol{x}} = \begin{pmatrix} \boldsymbol{p} \\ \boldsymbol{q} \end{pmatrix}, \tag{2.7}$$

and by taking $\boldsymbol{F}(\tilde{\boldsymbol{x}}, t)$ to be

$$\boldsymbol{F}(\tilde{\boldsymbol{x}}, t) = \boldsymbol{S}_N \cdot \frac{\partial H}{\partial \tilde{\boldsymbol{x}}}, \tag{2.8}$$

where $\boldsymbol{S}_N$ is the so called symplectic matrix given by

$$\boldsymbol{S}_N = \begin{bmatrix} \boldsymbol{O}_N & -\boldsymbol{I}_N \\ \boldsymbol{I}_N & \boldsymbol{O}_N \end{bmatrix} \tag{2.9}$$

where $\boldsymbol{I}_N$ is the N dimensional identity matrix, $\boldsymbol{O}_N$ is the $N \times N$ matrix of zeros, and

$$\frac{\partial H}{\partial \tilde{\boldsymbol{x}}} = \begin{bmatrix} \partial H/\partial \boldsymbol{p} \\ \partial H/\partial \boldsymbol{q} \end{bmatrix}. \tag{2.10}$$

From this vector notation we see how restricted the class of Hamiltonian systems is. In particular, a general system described as the form of (2.6) necessarily requires for the specification of all of the components of the vector function $\boldsymbol{F}(\tilde{\boldsymbol{x}}, t)$ being used, while by (2.8), if the system is Hamiltonian, it is specified uniquely by a single scalar function of $\boldsymbol{p}$, $\boldsymbol{q}$ and t which corresponds to the Hamiltonian.

One of the basic properties and a very important one of Hamilton's equations is that they preserve $2N$ dimensional volume in phase space. This follows by taking the divergence of $\boldsymbol{F}(\tilde{\boldsymbol{x}})$ in Equation (2.6), which gives

$$\nabla \cdot \boldsymbol{F} = \frac{\partial}{\partial \tilde{\boldsymbol{x}}} \cdot \boldsymbol{F} = \frac{\partial}{\partial \boldsymbol{p}} \left(- \frac{\partial H}{\partial \boldsymbol{q}} \right) + \frac{\partial}{\partial \boldsymbol{q}} \cdot \left(\frac{\partial H}{\partial \boldsymbol{p}} \right) = 0 \tag{2.11}$$

Thus, if we consider an initial closed surface S_0 in the $2N$ dimensional phase space and evolve each point that makes up the volume forward in time, we obtain at each instant of time t a new closed surface S_t which contains within it precisely the same $2N$ dimensional volume as the initial surface S_0. This follows as

$$\frac{d}{dt} \int_{S_t} d^{2N} \tilde{\boldsymbol{x}} = \oint_{S_t} \frac{d\tilde{\boldsymbol{x}}}{dt} \cdot d\boldsymbol{S} = \oint_{S_t} \boldsymbol{F} \cdot d\boldsymbol{S} = \int_{S_t} \frac{\partial}{\partial \tilde{\boldsymbol{x}}} \cdot d^{2N} \tilde{\boldsymbol{x}} = 0, \tag{2.12}$$

where the integrals $\int_{S_t} \cdots$ denote integration over the volume enclosed by S_t, $\oint_{S_t} \cdots$ denotes a surface integral over the closed surface S_t, and the third equality is a consequence of applying the divergence theorem to the closed integral [14]. From this result we can conclude that Hamiltonian systems do not posses what are called attractors in phase space. This incompressibility of phase space volumes for Hamiltonian systems is called Liouville's theorem [14] [16].

Perhaps we can say that the most important basic structural property of Hamilton's equations is that they follow a symplectic structure [14]:

$$\frac{d\tilde{\boldsymbol{x}}}{dt} = \boldsymbol{S}_N \cdot \frac{\partial H}{\partial \tilde{\boldsymbol{x}}}. \tag{2.13}$$

We can illustrate this geometry with the following arguments, if we consider three orbits and take them as if they are infinitesimally displaced from each other, $(\boldsymbol{p}(t), \boldsymbol{q}(t))$, $(\boldsymbol{p}(t) + \delta\boldsymbol{p}(t), \boldsymbol{q}(t)+\delta\boldsymbol{q}(t))$ and $(\boldsymbol{p}(t)+\delta\boldsymbol{p}'(t), \boldsymbol{q}(t)+\delta\boldsymbol{q}'(t))$, where $\delta\boldsymbol{p}$, $\delta\boldsymbol{q}$, $\delta\boldsymbol{p}'$ and $\delta\boldsymbol{q}'$ are infinitesimal N vectors, then the quantity represented by

$$\delta\boldsymbol{p} \cdot \delta\boldsymbol{q}' - \delta\boldsymbol{q} \cdot \delta\boldsymbol{p}', \tag{2.14}$$

which is to be called the differential symplectic area, will posses the characteristic to be independent of time,

$$\frac{d}{dt}(\delta\boldsymbol{p} \cdot \delta\boldsymbol{q}' - \delta\boldsymbol{q} \cdot \delta\boldsymbol{p}') = 0. \tag{2.15}$$

The differential symplectic area may also be written in vector notation as

$$\delta\boldsymbol{p} \cdot \delta\boldsymbol{q}' - \delta\boldsymbol{q} \cdot \delta\boldsymbol{p}' = \delta\tilde{\boldsymbol{x}}^\dagger \cdot \boldsymbol{S}_N \cdot \delta\tilde{\boldsymbol{x}}', \tag{2.16}$$

where † denotes transpose.

To derive the equality given by (2.15) we may differentiate (2.16) with respect to time and make use of the Equations (2.6) - (2.10):

$$\begin{aligned}
\frac{d}{dt}(\delta\tilde{\boldsymbol{x}}^\dagger \cdot \boldsymbol{S}_N \cdot \delta\tilde{\boldsymbol{x}}') &= \frac{d\delta\tilde{\boldsymbol{x}}^\dagger}{dt} \cdot \boldsymbol{S}_N \cdot \delta\tilde{\boldsymbol{x}}' + \delta\tilde{\boldsymbol{x}}^\dagger \cdot \boldsymbol{S}_N \cdot \frac{d\delta\tilde{\boldsymbol{x}}'}{dt} \\
&= \left(\frac{\partial \boldsymbol{F}}{\partial \tilde{\boldsymbol{x}}} \cdot \delta\tilde{\boldsymbol{x}}\right)^\dagger \cdot \boldsymbol{S}_N \cdot \delta\tilde{\boldsymbol{x}}' + \delta\tilde{\boldsymbol{x}}^\dagger \cdot \boldsymbol{S}_N \cdot \frac{\partial \boldsymbol{F}}{\partial \tilde{\boldsymbol{x}}} \cdot \delta\tilde{\boldsymbol{x}}' \\
&= \delta\tilde{\boldsymbol{x}}^\dagger \cdot \left[\left(\frac{\partial \boldsymbol{F}}{\partial \tilde{\boldsymbol{x}}}\right)^\dagger \cdot \boldsymbol{S}_N + \boldsymbol{S}_N \cdot \frac{\partial \boldsymbol{F}}{\partial \tilde{\boldsymbol{x}}}\right] \cdot \delta\tilde{\boldsymbol{x}}' \\
&= \delta\tilde{\boldsymbol{x}}^\dagger \cdot \left[\left(\boldsymbol{S}_N \cdot \frac{\partial^2 H}{\partial \tilde{\boldsymbol{x}} \partial \tilde{\boldsymbol{x}}}\right)^\dagger \cdot \boldsymbol{S}_N + \boldsymbol{S}_N \cdot \boldsymbol{S}_N \cdot \frac{\partial^2 H}{\partial \tilde{\boldsymbol{x}} \partial \tilde{\boldsymbol{x}}}\right] \cdot \delta\tilde{\boldsymbol{x}}' \\
&= \delta\tilde{\boldsymbol{x}}^\dagger \cdot \left[\left(\frac{\partial^2 H}{\partial \tilde{\boldsymbol{x}} \partial \tilde{\boldsymbol{x}}}\right)^\dagger \cdot \boldsymbol{S}_N^\dagger \cdot \boldsymbol{S}_N + \boldsymbol{S}_N \cdot \boldsymbol{S}_N \cdot \frac{\partial^2 H}{\partial \tilde{\boldsymbol{x}} \partial \tilde{\boldsymbol{x}}}\right] \cdot \delta\tilde{\boldsymbol{x}}' \\
&= 0,
\end{aligned} \tag{2.17}$$

where we have used the properties of the symplectic matrix $\boldsymbol{S}_N \cdot \boldsymbol{S}_N = -\boldsymbol{I}_{2N}$ (where $\boldsymbol{I}_{2N}$ is the $2N$ dimensional identity matrix), $\boldsymbol{S}_N^{\dagger} = -\boldsymbol{S}_N$ and noted that $\partial^2 H/\partial\tilde{\boldsymbol{x}}\partial\tilde{\boldsymbol{x}}$ is a symmetric matrix. We can also prove that the symplectic matrix $\boldsymbol{S}_N$ satisfies the following conditions [17] :

$$\boldsymbol{S}_N^{-1} = \boldsymbol{S}_N^{\dagger} = -\boldsymbol{S}_N \tag{2.18}$$

and

$$det(\boldsymbol{S}_N) = 1, \tag{2.19}$$

which can be obtained directly from Equation (2.9).

Symplectic systems present a wide variety of mathematical properties [17], but the one that is more relevant for this work, is that they conserve the volume on the $2N$ dimensional phase space, this means that symplectic dynamical systems follow the Liouville Theorem [14].

The fact that a Hamiltonian system conserves volume in the phase space has some consequences, we will highlight here the Poincaré Recurrence Theorem [18] [19]. When considering the movement of the system in a limited region of the phase space, which we denote as Γ, if we define a small area A within this region (REF FIGURA QUE NO HE HECHO), with volume $\Gamma_A < \Gamma$, we can obtain a set of time values $\{t_j\}$ for which the flow crosses this region from the inside out. The time intervals

$$\tau_j = t_{j+1} - t_j; \qquad j = 0, 1, 2, ... \tag{2.20}$$

are the Poincaré Cycles and t_j the Poincaré Recurrence Times.

FIGURA QUE NO HE HECHO DE LA REFERENCIA DE LOS CICLOS DE POINCARE

Poincaré proved that for a movement in a finite region of space in which the volume is preserved, the entire path sould return to a previously determined region (for example A in Figure FIGURA QUE NO HE HECHO) in a finite time and an infinite number of times. An exception occurs only if A is a zero dimension set [18] [19] [20].

Thus, in this chapter, some general properties of Hamiltonian dynamical systems have been described. This was made possible even without taking into account time evolution analysis of the systems, that is, their dynamics. In the coming sections, this question starts to gain space, focusing attention on some characteristics of its dynamics, more specifically when there is the presence of regular movement, chaos or a mixture of both.

2.2.1 Integrability in Hamiltonian problems

Another important topic related to Hamiltonian systems involves integrability, we will see in this subsection that integrability will naturally lead to the concept of chaos. As we have previously stated, in the case where the Hamiltonian of the system has no explicit time dependence, $H = H(\boldsymbol{p}, \boldsymbol{q})$, we have showed that Hamilton's equations imply that the Hamiltonian does not change in time $dH/dt = 0$ and the energy identified as the Hamiltonian $E = H(\boldsymbol{p}, \boldsymbol{q})$ is thus a conserved quantity. Therefore, orbits with a given energy E are restricted to lie on the $(2N-1)$ dimensional surface $E = H(\boldsymbol{p}, \boldsymbol{q})$ as a consequence of the dimensionality reduction due to the energy being a constant in time. A function $f(\boldsymbol{p}, \boldsymbol{q})$ is said to be a constant of motion of a system with Hamiltonian H if this quantity does not change in time even if $\boldsymbol{p}$ and $\boldsymbol{q}$ do. More generally, if we differentiate the function $f(\boldsymbol{p}, \boldsymbol{q})$ with respect to time, and assuming that there is no explicit time dependence for the Hamiltonian, if we make use of the hamilton's equations we obtain that

$$\frac{df}{dt} = \frac{d\boldsymbol{p}}{dt} \cdot \frac{\partial f}{\partial \boldsymbol{p}} + \frac{d\boldsymbol{q}}{dt} \cdot \frac{\partial f}{\partial \boldsymbol{q}} = \frac{\partial H}{\partial \boldsymbol{p}} \cdot \frac{\partial f}{\partial \boldsymbol{q}} - \frac{\partial H}{\partial \boldsymbol{q}} \cdot \frac{\partial f}{\partial \boldsymbol{p}} = 0 \tag{2.21}$$

We call the expression appearing on the right hand side of the second equality the Poisson bracket between f and H [16], and we shall abbreviate it as $\{F, h\}$. Using this definition, we can write a necessary a condition for a general function f to be a constant of motion when the Hamiltonian does not depend on time [18], for f to be a constant of motion then its Poisson bracket with the Hamiltonian must be equal to zero:

$$\{f, H\} = 0. \tag{2.22}$$

(We can show using this condition also that the Hamiltonian is correspondingly a constant of the motion since $\{H, H\} = 0$.)

For a system with N degrees of freedom to be integrable, in the Liouville sense, it is necessary for the system to posses N constants independent of motion $f_i(\bar{p}, \bar{q})$[1], with $i = 1, 2, ..., N$ in such a way that

$$\{f_i, H\} = 0 \tag{2.23}$$

and

$$\{f_i, f_j\} = \delta_{ij} \tag{2.24}$$

where δ_{ij} is the so called Kronecker delta [18]. To state it in another way, the vectors $\boldsymbol{v_i}$,

[1] If a constant cannot be described as a function of others, then it is called "independent" [14]

defined by

$$\boldsymbol{v_i} = \nabla f_i, \tag{2.25}$$

where $\nabla = (\partial/\partial q_1, ..., \partial/\partial q_N, \partial/\partial p_1, ..., \partial/\partial p_N)$ is the nabla operator of phase space, must be linearly independent at all the points in phase space [16]. If the conditions (2.23)-(2.25) apply to any i and j, then we say that the N constants of motion are in involution.

When an N-dimensional Hamiltonian system is integrable possesing N independent constants of motion, the topology of the surface on which its trajectories evolve in phase space is restricted to an N dimensional torus [18]. For the case $N = 2$, an orbit over a torus is shown in Figure (2.2)

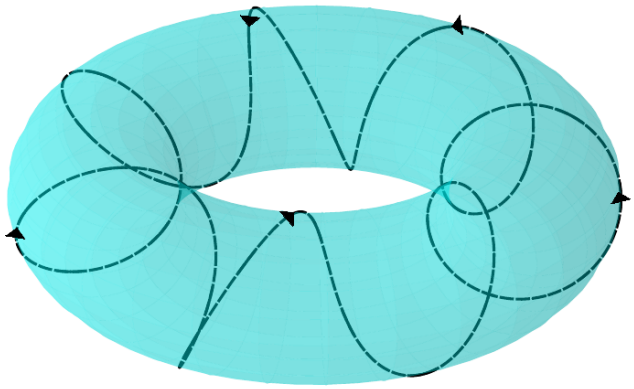

Figure 2.2: Trajectory on a torus for a bidimensional system with two constants of motion

We can state a simpler description of the movement of integrable Hamiltonian systems over the N dimensional torus by using the description in terms of the action-angle variables and the Hamilton-Jacobi equations, this formalism is explained in detail in Ref. [16]. In this framework a canonical change of variables $(\boldsymbol{p}, \boldsymbol{q}) \rightarrow (\tilde{\boldsymbol{p}}, \tilde{\boldsymbol{q}})$ is introduced such that the Hamiltonian $\tilde{H}$ depends only on $\tilde{\boldsymbol{p}}$ and not on $\tilde{\boldsymbol{q}}$. This way, the Hamilton's equations with the new Hamiltonian become

$$\frac{d\tilde{\boldsymbol{p}}}{dt} = -\frac{\partial \tilde{H}}{\partial \tilde{\boldsymbol{q}}} = 0 \qquad and \qquad \frac{d\tilde{\boldsymbol{q}}}{dt} = \frac{\partial \tilde{H}}{\partial \tilde{\boldsymbol{p}}} \tag{2.26}$$

and $H(\boldsymbol{p}, \boldsymbol{q})$ becomes a much simpler Hamiltonian depending only on the canonical momen-

tum, $\tilde{H}(\tilde{\boldsymbol{p}})$.

Using the action-angle variable formalism, we will write the components of the moment $\tilde{\boldsymbol{p}}$ and of the generalized coordinates $\tilde{\boldsymbol{q}}$ as

$$(\tilde{\boldsymbol{p}}, \tilde{\boldsymbol{q}}) = (\boldsymbol{I}, \boldsymbol{\theta}), \tag{2.27}$$

we will call $\boldsymbol{I}$ the action variable and $\boldsymbol{\theta}$ the angle variable, where the components of the action $\boldsymbol{I}_i$ are defined by [16]

$$\boldsymbol{I}_i = \frac{1}{2\pi} \oint p_i dq_i \qquad where \qquad i = 1, 2, ..., N. \tag{2.28}$$

This way, we are writing the components of the momentum $\tilde{\boldsymbol{p}}$ as being N constants of motion symplifying the Hamiltonian and at the same time satisfying Equation (2.26), since the time variation of a motion constant is zero.

In order to achieve the change of variables $(\boldsymbol{p}, \boldsymbol{q}) \rightarrow (\boldsymbol{I}, \boldsymbol{\theta})$, we use the generating function $S(\boldsymbol{I}, \boldsymbol{q})$ and the relations [16]

$$\boldsymbol{\theta} = \frac{\partial S(\boldsymbol{I}, \boldsymbol{q})}{\partial \boldsymbol{I}} \qquad , \qquad \boldsymbol{p} = \frac{\partial S(\boldsymbol{I}, \boldsymbol{q})}{\partial \boldsymbol{q}} \tag{2.29}$$

as these functions relate the "old" coordinates of the position $\boldsymbol{q}$ and the "new" momentum $\boldsymbol{I}$ [16]. With this relations, we will be able to construct the Hamiltonian function in terms of the action-angle variables, $\tilde{H}(I)$ which is independent of θ.

As said in the last paragraph, the new Hamiltonian is independent of $\boldsymbol{\theta}$ and the Hamilton equations (2.26), may be written as

$$\frac{d\boldsymbol{I}}{dt} = 0 \qquad and \qquad \frac{d\boldsymbol{\theta}}{dt} = \frac{\partial \tilde{H}(\boldsymbol{I})}{\boldsymbol{I}} \equiv \boldsymbol{\omega}(\boldsymbol{I}), \tag{2.30}$$

their solutions are easily calculated as

$$\boldsymbol{I}(t) = \boldsymbol{I}(0) \tag{2.31}$$

and

$$\boldsymbol{\theta}(t) = \boldsymbol{\theta}(0) + \boldsymbol{\omega}(\boldsymbol{I})t \tag{2.32}$$

where each angle variable is periodic with a period of 2π.

The second equation in (2.30) can be interpreted as an angular velocity vector specifying trajectories over the N dimensional torus [16], where $\boldsymbol{I}$ represents the radius of the trajectory

and $\boldsymbol{\theta}$ the angle of rotation. this fact is illustrated in Figure FIGURA QUE NO HE HECHO DE LA SECCION TRANSVERSAL DEL TORO for the case where $N = 2$. When we interpret $\boldsymbol{\omega}(\boldsymbol{I})$ as an angular velocity vector that specifies different paths over an N dimensional torus, we can interpret different types of motion along the torus' degrees of freedom, which may be periodic or quasi-periodic, depending on the ratio between these frequencies. If there is an N dimensional vector of integers $\boldsymbol{m} = (m_1, m_2, ..., m_n)$, such that

$$\boldsymbol{m} \cdot \boldsymbol{\omega} = 0, \tag{2.33}$$

except when $\boldsymbol{m}$ is a vector with all null components, the movement over the torus is a periodic movement and the ratio ω_1/ω_i is a rational number. In these cases, the orbits followed by the system close on themselves after m_1 cycles in θ_1, m_2 cycles in θ_2 and so on [14]. If by any chance the condition (2.33) is not satisfied and ω_1/ω_i is an irrational number, the motion of the system is called quasi-periodic and that orbit never returns to its starting point, this will result in the trajectory completely filling the surface of the torus [14].

When an integrable system begins to suffer the action of a disturbance of its trajectory, the tori whose ratio between frequencies is a rational or irrational number, behave in dfferent ways. The consequences of this disturbance on such tori are explained in detail by the KAM theorem, which we will describe next.

2.2.2 KAM Theorem

In the last subsections we introduced the necessary conditions for a system to be integrable. We also found that when we rewrite the Hamiltonian in terms of the constants of motion, especially in relation to the formalism of the angle-action variables, the system's movement can be described as to be limited to a rational or irrational N dimensional torus, depending on the frequencies of the motion. But where does the integrability of a Hamiltonian system go? Or yet, what happens to rational and irrational tori when an integrable Hamiltonian system is subject to a disturbance? The answers to these questions came with the rigorous mathematical work of Kolmogorov, Arnold and Moser (KAM) and with the numerical studies developed on chaos and integrability after the advent of computer. The results obtained by Kolmogorov, Arnold and Moser became known as the KAM Theorem. The deduction of the theorem will not be detailed here, as it is ourside the scope of this work, only its results will be presented.

To describe the KAM theorem, we consider a disturbed Hamiltonian system, written in

terms of the action-angle variables as

$$H(\boldsymbol{I}, \boldsymbol{\theta}) = H_0(\boldsymbol{I}) + \epsilon H_1(\boldsymbol{I}, \boldsymbol{\theta}), \tag{2.34}$$

where $H_0(\boldsymbol{I})$ is the integrable Hamiltonian, $H_1(\boldsymbol{I}, \boldsymbol{\theta})$ the perturbation and $(\boldsymbol{I}, \boldsymbol{\theta})$ the action-angle variables of perturbed system.

The main idea of the KAM Theorem is to consider the effect of the disturbance on invariant Tori [2] instead of the trajectories in the phase space [18]. In this way, we will divide the discussion into two cases, the Rational Torus and the Irrational Torus. We will se that many tori survive small disturbances, while others destroy themselves, giving rise to chaotic orbits, new tori and also elliptical and hyperbolic points.

2.2.3 Rational Tori

We call Rational Tori those whose ratio between the frequencies given by Equation (2.30) is a rational number. As a result of the action of the disturbance, these Tori are destroyed and it does not matter how small the values of ϵ are [14]. Due to the destruction of the Rational Torus, there is the appearance of an equal number of fixed elliptic and hyperbolic points. This result is known as the Poincaré Birkhoff theorem [21] . The number of fixed points that appear depends on the ratio between the frequencies of the rational torus. If we call $R = \tilde{p}/\tilde{q}$ the torus rotation number, where $\tilde{q}$ represents the largest number of cycles performed on the torus before the path returns over itself, then, due to the disturbance, there will appear an equal or multiple number of $\tilde{q}$ of elliptical points and hyperbolic points [14]. Figure (FIGURA QUE NO HE HECHO DEL TORO RACIONAL PERTURBADO POCAMENTE) illustrates a case where $\tilde{q} = 3$ and $\tilde{q} = 4$ in a Poincaré section for a system with $N = 2$.

These elliptical and hyperbolic points that result from the breakdown of the rational torus due to the perturbation, they remain fixed points of the disturbed system and with the same period $\tilde{q}$ of the rational torus [21]. The difference between the two points is in the way initial conditions close to them behave. Next to fixed elliptical points, new curves appear similar to those that existed before the perturbation, which we call KAM curves, some of which are rational and others irrational. Such fact is presented inside the box on Figure (FIGURA ANTERIOR LA PARTE B TIENE UNA CAJA CERRADA DE UN PUNTO ELIPTICO). When these rational KAM curves that appeared due to the action of the disturbance are

[2] A torus is called invariant if once the motion of the system starts on itm the motion will remain on it [14].

destroyed, other elliptical and hyperbolic points will appear, surrounded again by rational and irrational KAM curves and so on [14].

Orbits enerated near hyperbolic points, can have different behaviors, because hyperbolic points, also known as saddle points, have stable directions or varieties, those that move to the fixed point, or unstable, those who move away from it [14]. If we follow the varieties, moving away from a fixed point, they will usually present homoclonic or heteroclonic intersections, which occur when unstable varieties from the same point cross over themselves or from two different points intersect at different points, respectively [14]. Figure (REF FIGURA QUE NO HE HECHO DE LOS ENREDAMIENTOS HOMOCLINICOS) represents these crossings for a single point and for two distinct hyperbolic points.

Thus, the destruction of the rational torus not only generates stable elliptical points, but also generates hyperbolic points, which are responsible for the chaotic movement, which is always trapped by the KAM curves that haven't been "broken" [14], at least for an $N = 2$ case. As these curves begin to "break", more and more chaotic regions are appearing, completely filling with points the allowed region of the Poincaré section. We will now see what is the sequence in which the irrational torus gives rise to the elliptical and hyperbolic points.
FIGURA
QUE
NO
HE
HECHO
DE
LOS
PUNTOS
Y
CRUZAMIENTO
HOMOCLINICO

2.2.4 Irrational Tori

When an integrable system is disturbed, the KAM Theorem guarantess the existence of a torus in the phase space, if te conditions below are met:

1. The torus' linear frequencies of the integrable system are independent [21], that is, we hae a torus whose ratio between the frequencies is an irrational number.

2. The perturbation is a smooth function [21] (a sufficient number of derivaties of H_1).

3. Initial conditions are sufficiently far from the rational tori [21].

With the above conditions satisfied, the KAM Theorem guarantess the existence of deformed torus, with the same topology as the unperturbed torus, in the vicinity of te irrational torus of the system in the non-perturbed. These tori that appear deformed after the perturbation are called the KAM Tori.

The that the irrational torus must be sufficiently far from the rational torus, for the existence of the KAM Tori, implies that the more irrational the ratio between the frequencies of the non-perturbed tori, the easier it is for the KAM Tori to appear [21].

The idea of more irrational numbers can come with the help of number theory. An irrational number R can be represented as an infinite continuous function [14]:

$$R = a_1 + \frac{1}{a_2 + \frac{1}{a_3 + \frac{1}{a_3 + \cdots}}} \tag{2.35}$$

where the a_i's are integer numbers. However, if the integers a_i's for $i \geq k$ are equal to one, this irrational number is called "noble" [22]. The "most irrational" numer that exists is consequently the most "noble" of them all [22], and it is the golden ratio

$$R = \frac{(\sqrt{5} - 1)}{2} \tag{2.36}$$

When the most "noble" number of all is related to the irrationality of a KAM Tori, it will be the last one to be destroyed as the intensity of the perturbation is increased. However, if it is not present, the last KAM Tori to be destroyed will be the one with the most "noble" number [22].

In general, the effect of the perturbation on an integrable system can be summarized as follows: When the disturbance begins to act on the integrable system, many tori of the integrable system are slightly deformed and survive (Irrational Tori), while others are destroyed (Rational Tori). Regions close to the tori that were not destroyed by the perturbation are occupied by new irrational orbits, elliptical points, hyperbolic orbits and chaotic orbits. As the disturbance increases, the irrational tori destroy themselves, the last one to be "destroyed", is the one that has the value of the ratio between the frequencies as a "more noble" number.

When the perturbation on the integrable system breaks all tori, including the "noblest", the system starts to present characteristics such as ergodicity, drops of correlations, etc...

2.3 Symplectic Integrator

As we said previously, symplecticness is a very important property of the Hamiltonian systems, this feature is also present on numerical integration and the need of symplectic integrators algorithms arise. Numerical integrators, generally speaking, are numerical mappings of the differential equations, most of the times these mappings are nonsymplectic. Applying nonsymplectic algorithms to hamiltonian problems tend to show solutions where the area in phase space is not conserved. We show this problem in Figure (2.3) which illustrates this issue by taking the fundamental problem of the harmonic oscillator and integrating its equations of motion using the standard first order differential equation solver known as the Euler method (which is a nonsymplectic integrator) and also a first order symplectic algorithm known as the Verlet Leapfrog method[23] [24]. The general problem of nonsymplectic algorithms and hamiltonian problems is their tendency to not conserve the energy in time, we see this feature on Figure (2.3) where the trajectory of the nonsymplectic algorithm drifts in time as a consequence of energy being transferred to the system due to numerical error.

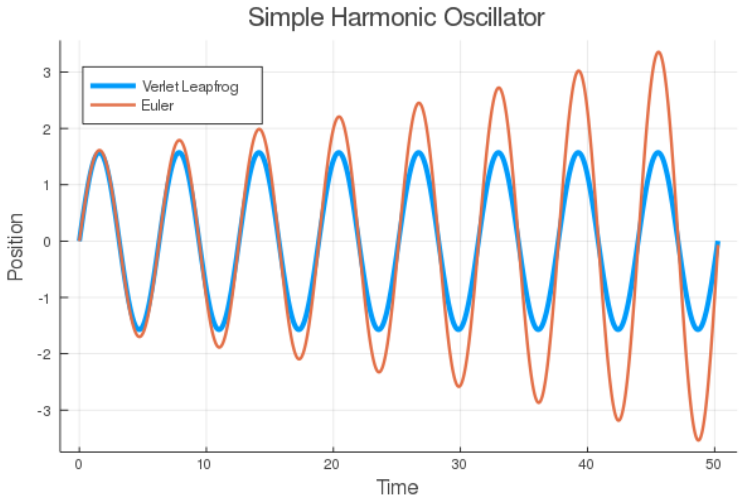

((a)) Position dynamics

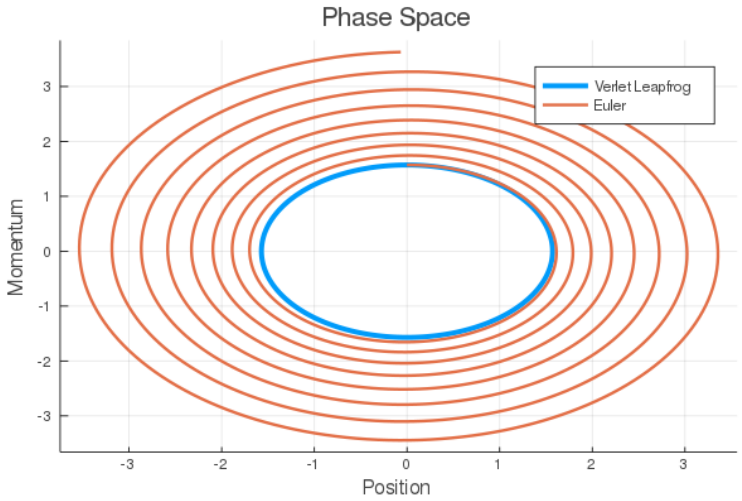

((b)) Phase space dynamics

Figure 2.3: Euler non symplectic integrator compared to symplectic Verlet Leapfrog method

This failure of mimicking well known Hamiltonian dynamics suggested the consideration of schemes that generate a symplectic mapping Ψ when applied to Hamiltonian problems, this mapping does not necessarily need to be perfect but at least really close to the symplectic manifold of the original problem. Such methods are called symplectic or canonical. Early references on symplectic integration are [25][26][27][28][29], but the first notions and ideas about the symplectic structure regarding integration techniques dates back to DeVogelaere in 1956 [30].

2.3.1 Importance of symplecticness in an integrator

When talking about a domain Ω possesing a symplectic structure Λ, taking a smooth hamiltonian function gives rise to a hamiltonian system of differential equations known as the Hamilton equations. This domain we are talking about reffers to the phase space of the hamiltonian system. If we consider a time step $h > 0$, we can build a numerical scheme to solve these differential equations by using the function $\Psi : \Omega \to \Omega$ that depends on the step size h and the hamiltonian function of the system H. Then given an initial condition on the phase space (p_0, q_o) we can estimate an aproximation to the solution at time nh by iteratively applying the function Ψ

$$(p_{n+1}, q_{n+1}) = \Psi(p_n, q_n). \tag{2.37}$$

We may call the maping of the function Ψ a symplectic integrator if the maping conserves the symplectic structure of a system, $\Psi\Lambda = \Lambda$[31][32][25] [26]. A symplectic integrator is then an integrator whose solution resides on a symplectic manifold. Because of discretization error, when it is solving a Hamiltonian system it doesn't get exactly the correct trajectory on the manifold. Instead, that trajectory itself is perturbed by $\mathcal{O}(\Delta h^n)$ for the order n from the true trajectory where Δh is the timestep difference. Because of these arguments there is a linear drift due to numerical error of this trajectory over time. Normal integrators tend to have a quadratic (or more) drift, and do not have any good global guarantees about this phase space path, it only guarantees the path in a local sense.

Therefore symplectic integrators tend to capture the long-time patterns better than normal integrators because of this lack of drift in the trajectory and this almost guarantee the periodicity of certain problems at least for the desired time span.

2.3.2 Conservation of constants of motion

As we have seen previously, when one uses a symplectic integrator of order n what you do is to solve in an exact way the evolution of the system, but not using the hamiltonian H but one softly perturbated as $\tilde{H} = H + \epsilon H_1$, where $\epsilon = t^n$ and $H_1 = H_1^0 + hH_1^1 + h^2H_1^2 + ...$ If what we really want to obtain is a qualitative information of the behavior of the system, we can expect that if ϵH_1 is sufficiently small, the system will evolve in a very similar way for $\tilde{H}$ as for H.

Consider now a system that has m independent constants of motion J_i where $i = 1, ..., m$, this means that for every J_i it satisfies the condition of a null poisson bracket with the hamiltonian as $\{H, J_i\} = 0$. As the integrator is solving in an exact way the evolution due to the hamiltonian $\tilde{H}$, it will follow that the constants of motion, in general, will not be

constant as they will not have a null poisson bracket, in principle, with this new hamiltonian. Nonetheless, the following is obtained

$$\{\tilde{H}, J_i\} = \{H + \mathcal{O}(h^n), J_i\} = \mathcal{O}(h^n). \tag{2.38}$$

Despite some exceptions, the constants of motion J_i will not be constant along the evolution of the system, but they will disagree to being it in the same order as the energy does. Therefore, for an efficient integrator with high order precision the constants of motion will certainly be constant along the dynamical trajectory.

2.3.3 Chaos and integrators

Numerical chaos has been a very interactive branch of study for many years specially ever since numerical computations where able to be performed on computers . As we have shown, numerical stability of differential equations is very sensitive to systems involving chaos, even the slightest difference on the floating point error gives rise to diverging trajectories in phase space, this makes chaotic systems very interesting problems numerically speaking. As we know, floating numbers that computer algorithms work with have a finite value for decimals, when computing a solution of a differential equation using a given algorithm computers truncate this decimals leaving some round-off error. These truncations are not overseen by chaotic systems, chaotic systems have the nature of amplifying the slightest disturbance of the system into an observable result, this means that numerical truncations on floating point numbers have long term consequences when interpreting what we consider the solution. Therefore it is necessary to take into account these considerations regarding round-off precision when solving a chaotic system.

Numerical integrators and chaos consequently gather on an exotic dance of conditions to consider, on the one hand it is important for integrators to have a high order of accuracy by using intermediate steps before computing a definitive step on the trajectory of the solution and it is also important to have a small enough integration step to manage sensibility for the trajectory; on the other hand, error propagation of the floating point decimal truncation everytime the integrator performs an operation discourages all the effort put into calculating derivatives using intermediate steps and raises the question on what is the important aspect to consider. The answer is often unknown, solving these numerical problems with optimal efficiency is truly a very complicated task for the majority of chaotic problems[33].

Some chaotic problems might require calculations with a precision not always performed by usual codes and computers and if this is achieved the computational resources needed to

arrive to a fixed point solution might be way to big to calculate [34].

For the case of Hamiltonian systems, if the system is perturbed by a certain degree, the KAM theorem gives us information about the quasiperiodic orbits that will arise in the dynamics of the system[35][36][37]. If a normal hamiltonian system is perturbed to a certain degree the problem may become non integrable in the sense of its orbits not easily represented by analytical functions, this is where numerical integrators play a huge role on determining the dynamics of these systems. Therefore correct numerical algorithms that map the hamiltonian dynamics in a correct way in systems including chaos plays a very important role in the area of numerical differential equations problems. This means that symplectic algorithms to solve the differential equations for Hamiltonian systems with these properties arise as a very useful tool due to the conservation of the important quantities of the overall system.

2.4 Randomness in classical and quantum mechanics

Randomness and chaos share similarities physically speaking, they amplify any type of noise from the microscopical degrees of freedom and show them visible in the outcome of the dynamics of the systems. The idea to achieve true randomness on experiments or random number generators is a dream for many experimentalists, but the true situation is that most of the times, classically you can't have the perfect un-biased scenario of randomness. One great example is illustrated by Diaconis et al. [38] where very precise measurements and theroretical descriptions are applied to the commonly known random event of the coin toss. The outcome of this research is that for natural flips the result of the coin is biased to come up as started 51% of the times. Another example of a physical method to come up with random numbers is related to optical chaos [39][40], it has has a high potential to physically produce high-speed random numbers due to its high bandwidth and large amplitude. A prototype of a high speed, real-time physical random bit generator based on a chaotic laser was built in 2013 [41].

Determinism defined as the property of events to be determined completely by previously existing causes is an important concept concerning classical mechanics, given the equations of motion of a system, we know in an exact way the state of the system in a future time with arbitrary precision. Chaotic systems are very sensitive to small changes on the initial conditions and they are often missunderstood as random, but as we have previously described, chaotic systems do not exhibit random behavior in the sense that it can be at any place located in phase space but we have shown that it certainly remains conditioned by a certain degree

to the motion on the KAM tori giving place to quasiperiodicity.

Another important example of randomness in classical physics is present for example in fluid and molecular dynamics, where the numbers of degrees of freedom is of the order around Avogadro's number, due to this big number it is convenient to treat systems in a probabilistic way instead of following the dynamics of each of the particles that compose the system. This is therefore a randomness in the dynamics but given as a consequence of the choice to not follow explicitly each particle, one could say it is a randomness on purpose. This doesn't mean that these types of systems can't be described and simulated without a good accuracy, on the contrary, the methods to describe these types of systems are very sophisticated and a very interactive branch of research[42][43].

On the other hand, quantum mechanics seems to have fundamental randomness in its roots, measurements are regarded as probability measurements of the system to be in a determined state. The Born's interpretation of the quantum mechanics of the wave function implies that we can count only on a probabilistic description of reality, therefore quantum mechanics is inherently probabilistic [44]. Randomness in quantum mechanics is also regarded to be due to the interaction of a measurement apparatus and an environment with the initial pure states. This is consistent and parallel to the modern way of intepretations of the collapse of the wave functions and the quantum measurements [45] [46][47].

It is important for us to talk about the experiment to measure a spin component along a direction. If we take the z component as an example similar to the Stern-Gerlach experiment [48], in this experiment the particles before the measurement are regarded to be in a neutral state along the z component, after the particles go through the inhomogeneous magnetic field the spin aligns along a direction of the z component and gets deflected along this direction. The result of the experiment is seen in a screen where two clouds of particles are seen, one in the upper location and one in the lower one. The counts of particles on each cloud is the same in both cases, this translates as the probability of the particles to be aligned along certain direction is the same. Particles then have a completely random probability to the aligned along certain direction, this idea can be compared with the one of the coin toss, only two possible outcomes of the measurement. There is a big difference between both pictures besides one being classical and the other one quantum, it is that the coin toss is not truly random as it depends strongly on the initial conditions on how the coin toss is made meanwhile the spin measurement seems to be totally random as long as the particle is initially in a non-commuting state with the z component of the spin. This idea is the one we are going to exploit on the next chapters and explore a little bit the grounds of the environment and its role of introducing bias to the outcome of the measurements.

CHAPTER 3

Double well and finite heat bath

In this chapter we will use a model to test the interaction between a particle on a double well potential coupled bilinearly on position with a bath consisting of harmonic oscillators. This model is initially chaotic following the rules we have stated on the previous chapters regarding chaotic motion. The difference here with the previous chapters is that we will increase the number of degrees of freedom in the whole system by increasing the number of harmonic oscillators in the heat bath[49].

The main results of this chapter are related to the theory of dissipative dynamics in open systems but with a finite number of oscillators in the heat bath. We will play with different parameters of the heat bath such as energy and frequencies following this matter.

3.1 Double well as a two level system

3.1.1 Quantum modeling for continuous variables

3.1.2 Heat bath proper modeling

3.2 Dynamics of the system

In this section we will describe the mathematical properties of the system as a hamiltonian problem. We will study the different dynamics the system will have as afunction of its parameters, we will treat the heat bath as a finite heat bath instead of the common infinite heatbath in the microscopic theory of dissipation in Langevin dynamics. We will evidence here that even if the heat bath is not infinite, it will mimic the dissipation of an infinite heat

bath.

3.2.1 Hamilton equations of motion

The model of a particle coupled to a heat bath that we will study here is described by the following hamiltonian:

$$H(p,x;\mathbf{P},\mathbf{X}) = H_S + H_B + H_{SB} \tag{3.1}$$

Where the hamiltonian for the central system (S) can be viewed as a particle of mass m moving in a double well potential of quartic nature. The corresponding hamiltonian reads as

$$H_S = \frac{p^2}{2m} - a\frac{x^2}{2} + b\frac{x^4}{4}, \tag{3.2}$$

where p is the momentum of the particle, q is te position of the particle, and a, b are parameters that change the shape of the potential.The hamiltonian for the bath (B) is described as a set of harmonic oscillators

$$H_B(\mathbf{P},\mathbf{X}) = \sum_{n=1}^{N}\Big(\frac{P_n^2}{2M_n} + M_n\omega_n^2\frac{X_n^2}{2}\Big), \tag{3.3}$$

each oscillator n posses position X_n, momentum P_N, frequency ω_n and mass M_n. The last term of the hamiltonian consists on the interaction term where the system and bath positions are coupled bilinearly according to

$$H_{SB}(p,x;\mathbf{P},\mathbf{X}) = -x\sum_{n=1}^{N} g_n X_n + x^2\sum_{n=1}^{N}\frac{g_n^2}{2M_n\omega_n} \tag{3.4}$$

The last term here acts as a counter term whose job is to renormalize the potential when the interaction between the oscillators is present. This hamiltonian is often called the Caldeira-Leggett hamiltonian [50].

The hamilton equations for this hamiltonian can be separated in the two parts, the particle and the heat bath. The hamilton equations of the particle read as

$$\dot{p} = \frac{-\partial H}{\partial x} = ax - bx^3 + \sum_{n=1}^{N} g_n X_n - x\sum_{n=1}^{N}\frac{g_n^2}{M_n\omega_n^2}, \tag{3.5}$$

$$\dot{x} = \frac{\partial H}{\partial p} = \frac{p}{m}. \tag{3.6}$$

For the heat bath we find that the equations of motion for each of the n oscillators are

given by

$$\dot{P}_n = \frac{-\partial H}{\partial X_n} = -x g_n - M_n \omega_n^2 X_n \tag{3.7}$$

$$\dot{X}_n = \frac{\partial H}{\partial P_n} = \frac{P_n}{M_n} \tag{3.8}$$

From these equations we can calculate the frequency of small oscillations for the double well potential, we proceed by taking the the potential given as

$$V(x) = -\frac{1}{2}ax^2 + \frac{1}{4}bx^4, \tag{3.9}$$

the equilibrium points are located where the potential V is minimum or maximum, this is when the following condition is satisfied

$$\frac{d}{dx}V = 0 \rightarrow x(bx^2 - a) = 0. \tag{3.10}$$

The solutions for this equation are $x = 0, \pm\sqrt{\frac{a}{b}}$, where $x = 0$ is an unstable equilibrium point and $x = \pm\sqrt{\frac{a}{b}}$ are stable equilibrium points

We proceed to perform a Taylor expansion around a stable equilibrium point say $x_0 = \sqrt{\frac{a}{b}}$ as

$$V(x_0 + \epsilon) = V(x_0) + U'(x_0)\epsilon + \frac{1}{2}V''(x_0)\epsilon^2 + ... \tag{3.11}$$

The first term on the right side is a constant term, this means it can be ignored. The second term is equal to zero due to the fact that $V'(x_0) = 0$ is the condition for the stable minimum. The third term will be according to the result of $V''(x_0) = \frac{1}{2}(-a + 3bx^2)|_{x=x_0}$, this results in the following expansion

$$V(x_0 + \epsilon) \approx \frac{1}{2}(2a)\epsilon^2. \tag{3.12}$$

This potential is the same expression of a harmonic oscillator potential with a spring constant of $k = 2a$ (compared with the harmonic oscillator potential $V_{HO} = \frac{1}{2}kx^2$). This means that the frequency of small oscillations around the stable minimum is given by

$$\omega = \sqrt{\frac{k}{m}} = \sqrt{\frac{2a}{m}} \tag{3.13}$$

For the case of the particle coupled to the heat bath we can do the same analysis and see the role of the counter term in the hamiltonian resulting in the same results as above. The

equilibrium points of the whole hamiltonian must satisfy the following condition

$$\frac{d}{d\mathbf{x}}H = 0 \rightarrow \frac{d}{dx}H = 0 \quad , \quad \frac{d}{dX_n}H = 0. \tag{3.14}$$

Evaluating the derivatives we arrive to the following equations

$$x(bx^2 - a) - \sum_{n=1}^{N} g_n X_n + \sum_{n=1}^{N} \frac{x g_n^2}{M_n \omega_n} = 0 \quad , \quad x g_n = M_n \omega_n^2 X_n \tag{3.15}$$

where the right hand side equation will provide the constraint to retrieve the original conditions of equilibrium for the potential on the right hand side

$$x(bx^2-a)-\sum_{n=1}^{N} g_n X_n+\sum_{n=1}^{N} \frac{x g_n^2}{M_n \omega_n} = x(bx^2-a)-\sum_{n=1}^{N} g_n X_n+\sum_{n=1}^{N} g_n X_n = x(bx^2-a) = 0. \tag{3.16}$$

We can also calculate the height of the potential barrier (the difference between the height of the unstable equilibrium with the stable equilibrium), we can do this by insterting one of the minima on equation (3.9):

$$V(\sqrt{\frac{a}{b}}) = -a\frac{a}{2b} + b\frac{a^2}{4b^2} = \frac{-a^2}{2b} + \frac{a^2}{4b} = -\frac{a^2}{4b}, \tag{3.17}$$

For this particular situation the unstable equilibrium is located at the 0 height, meaning that in general the height of the potential barrier will be the difference between the unstable and the equilibrium point given as

$$PB(a, b) = \frac{a^2}{4b} \tag{3.18}$$

3.2.2 Poincaré surface plots for finite heat bath

We start the numerical experiments of this model with only one oscillator coupled to the particle of the central system. This very simple model already exhibits the traits and characteristics of a chaotic system, this is due to the barrier of the unstable equilibrium position. We can illustrate this by picturing the particle moving on the double well potential without any coupling with the heat bath, if the particle has enough energy, it will move freely between the two wells, otherwise it will orbit around one well. This can be seen in two different ways, the first one is by looking at the potential part of the hamiltonian of each part of the whole system i.e. the quartic potential and the harmonic oscillator potential, plotting each potential along an axis we can see the contours of energy for the dynamics of the system.

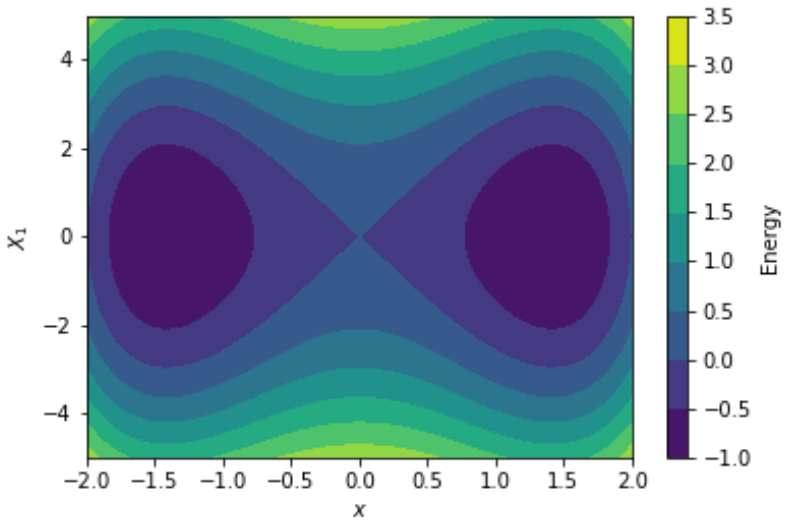

Figure 3.1: Energy contour of the double well potential on the x axis and the harmonic oscillator potential on the y axis for $m = 1$, $a = 2$, $b = 1$, $\omega_1 = 1.5$, $M_1 = 0.1$ and $g_1 = 0$

In Figure (3.1) we see that as the dynamics is uncoupled, the particle moves freely on the double well potential and the harmonic oscillator doesn't really changes its motion.

Following this representation we can observe the perturbation induced by the harmonic oscillator when we "turn on" the coupling between the two systems, for a coupling of $g_1 = 0.1$ it is already evident that shape of the whole potential suffers a shearing effect:

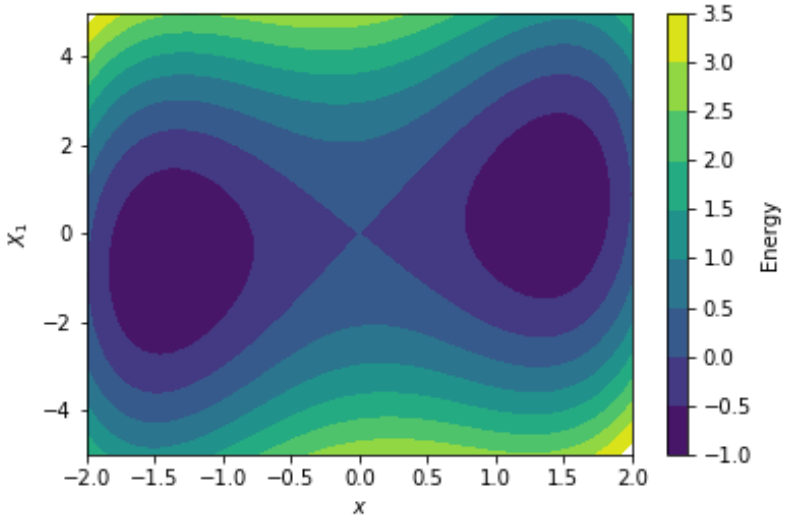

Figure 3.2: Energy contour of the double well potential on the x axis and the harmonic oscillator potential on the y axis for $m = 1$, $a = 2$, $b = 1$, $\omega_1 = 1.5$, $M_1 = 0.1$ and $g_1 = 0.1$

This means that independently of the initial conditions of the particle, the motion will be certainly affected by the presence of the potential due to the harmonic oscillator.

Now that we have seen a visual representation of the system without solving the equations of motion of the system, it is necessary to take a look at the specific dynamics of the system numerically by using a symplectic integrator. The integrator of our choice is the Calvo Sanz-Serna 4th order symplectic integrator [51][52][53], we use a timestep defined by $dt = 0.05 * T$ where $T = \frac{2\pi}{\omega_t}$ is the period of a harmonic oscillator of frequency $\omega_t = 12$. Here we set up different initial conditions for the particle along its phase space, the position of the oscillator always to start at $X_1 = 0$ and fixed the energy (twice the energy of the potential barrier between the wells here) as a constraint to be followed by the initial momentum of the oscillator. Each point of the Poincaré section is registered as the event when the oscillator crosses its equilibrium position $X_1 = 0$ with a possitive momentum. We will take a number of initial conditions along the phase space of the particle and start to increase the coupling to see the behavior of the orbits in the phase space of the particle.

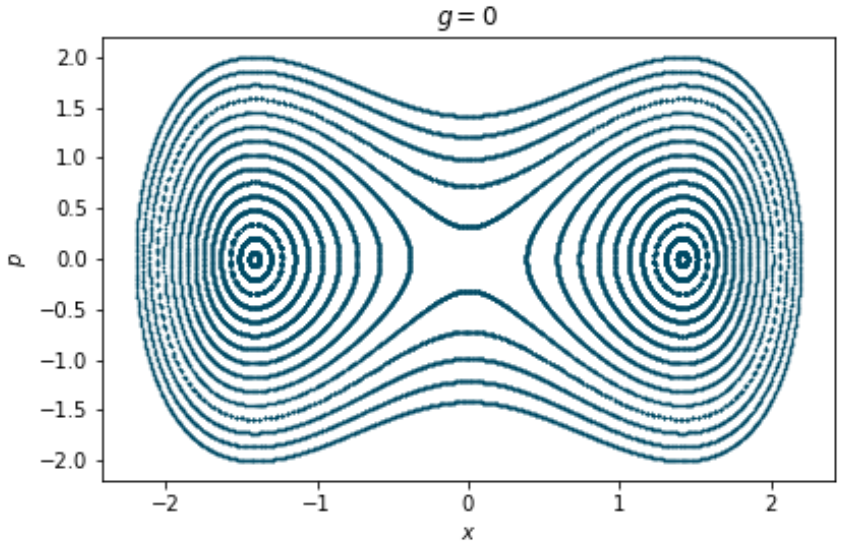

Figure 3.3: Poincaré surface plot for the particle phase space for $m = 1$, $a = 2$, $b = 1$, $\omega_1 = 1.5$, $M_1 = 0.1$ and $g_1 = 0$

In Figure (3.3) we start with $g_1 = 0$ and see that the orbits on the phase space of the particle are closed, the particle is totally unaware of the harmonic oscillator's potential. Now we will slowly start to "turn on" the coupling between the systems.

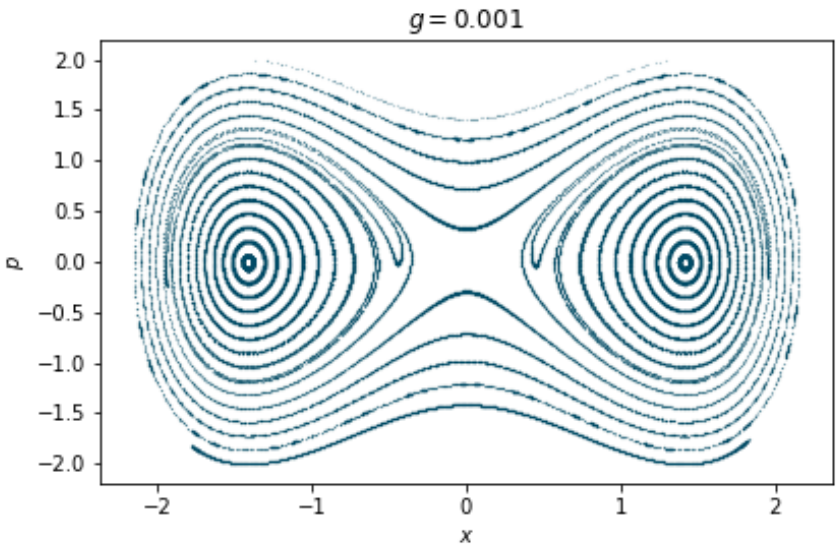

Figure 3.4: Poincaré surface plot for the particle phase space for $m = 1$, $a = 2$, $b = 1$, $\omega_1 = 1.5$, $M_1 = 0.1$ and $g_1 = 0.001$

As soon as there is coupling present in the dynamics of the system the orbits start to destroy progresively as we can see in this Figure (3.4).

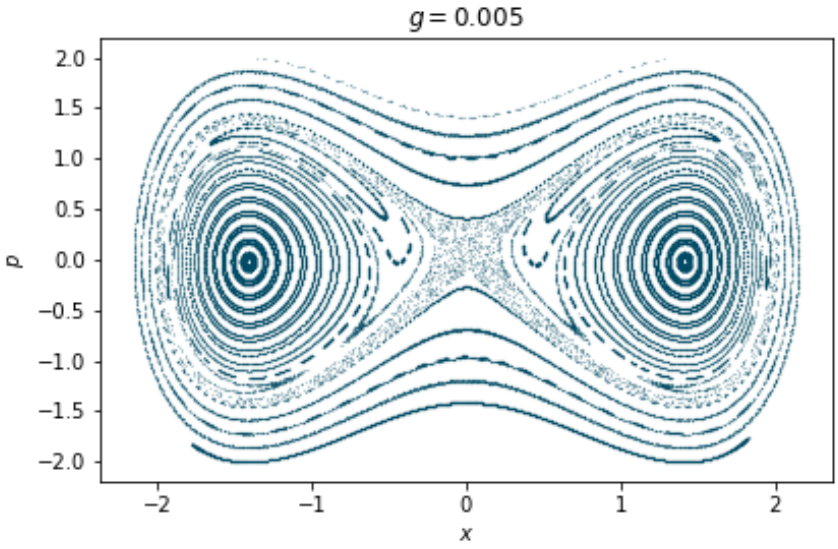

Figure 3.5: Poincaré surface plot for the particle phase space for $m = 1$, $a = 2$, $b = 1$, $\omega_1 = 1.5$, $M_1 = 0.1$ and $g_1 = 0.005$

The section of phase space where we start to see pure chaos at first is when the energy of the particle is very close to the energy of the barrier between the two wells as we can see in

Figure (3.5), this particular behavior around this points is of particular interest for our case as we will later use the unstable equilibrium position as the initial condition for the particle.

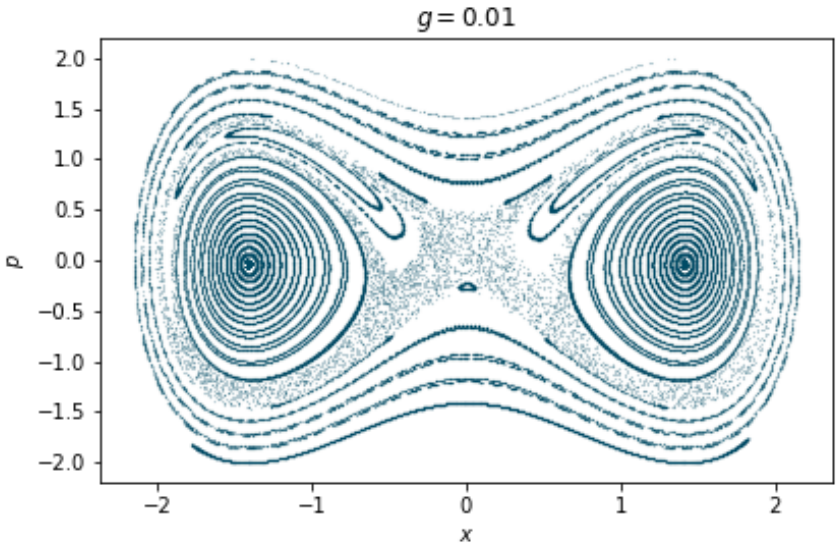

Figure 3.6: Poincaré surface plot for the particle phase space for $m = 1$, $a = 2$, $b = 1$, $\omega_1 = 1.5$, $M_1 = 0.1$ and $g_1 = 0.01$

As we continue to increase the coupling strength we progress on the destruction of the orbits and approach to a more chaotic behavior.

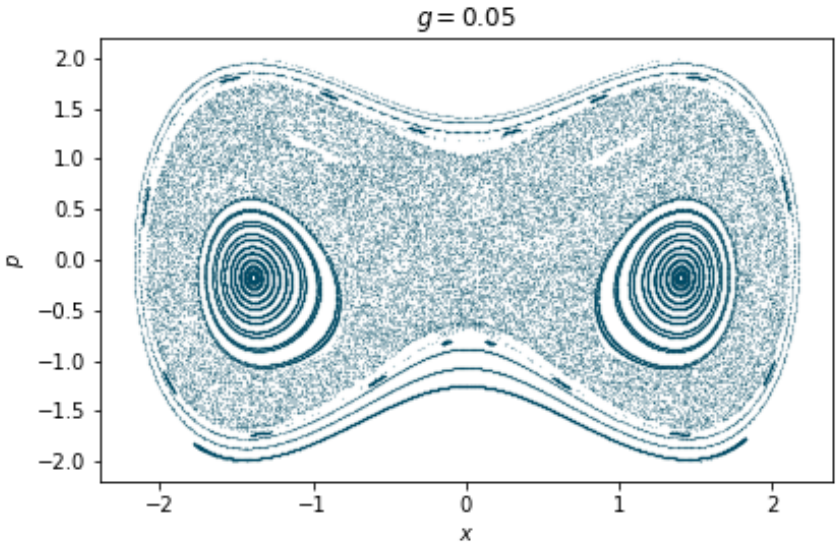

Figure 3.7: Poincaré surface plot for the particle phase space for $m = 1$, $a = 2$, $b = 1$, $\omega_1 = 1.5$, $M_1 = 0.1$ and $g_1 = 0.05$

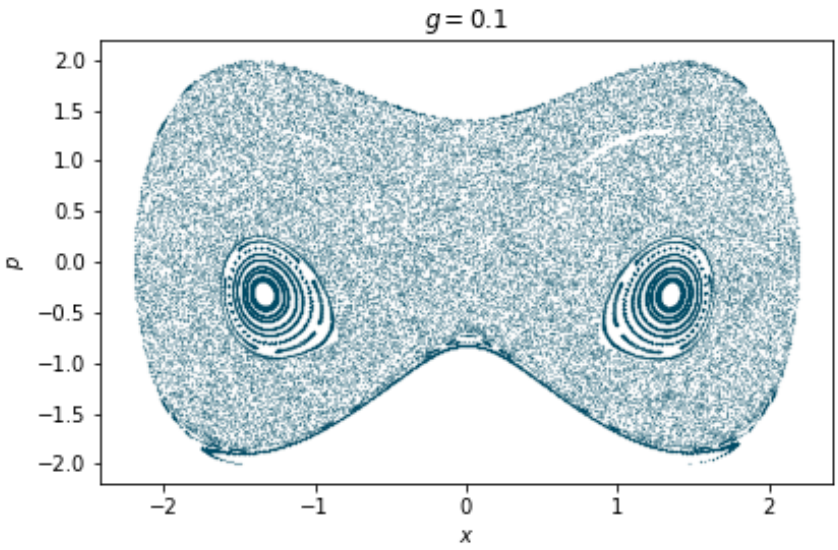

Figure 3.8: Poincaré surface plot for the particle phase space for $m = 1$, $a = 2$, $b = 1$, $\omega_1 = 1.5$, $M_1 = 0.1$ and $g_1 = 0.1$

Finally in Figure (3.8) we arrive to the coupling we used for Figure (3.2) $g = 0.1$. As we can see from the poincaré section, the overall behavior of the system is very chaotic except for the stable islands very near to the condition of the particle to have small energy located near to the stable equilibrium points with a small momentum. Comparing these two pictures we can see that even if the shearing behavior observed in the contour plots can barely be noticed, the dynamics of the system is almost completely chaotic.

Just for illustration we calculated the poincare section for $g = 0.2$ to show that the behavior of pure chaos continues to increase, this is shown in Figure (3.9).

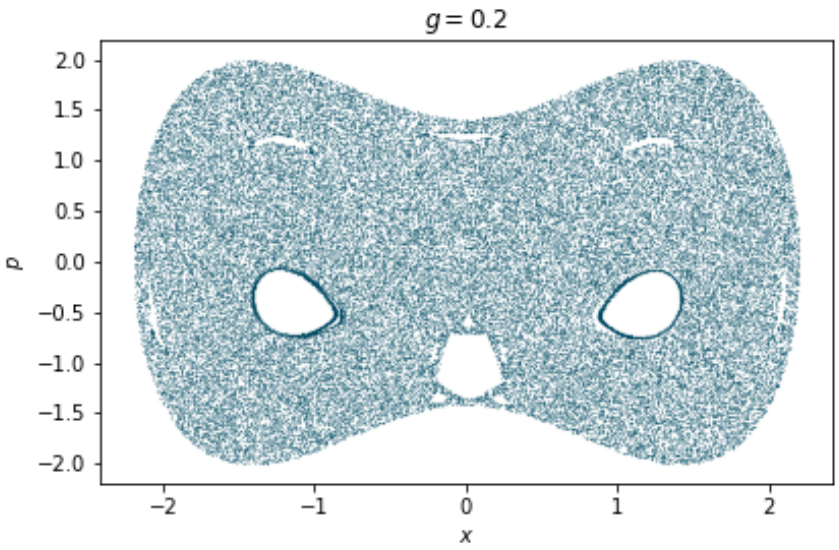

Figure 3.9: Poincaré surface plot for the particle phase space for $m = 1$, $a = 2$, $b = 1$, $\omega_1 = 1.5$, $M_1 = 0.1$ and $g_1 = 0.2$

3.2.3 Dynamics for 1 oscillator

We have seen in the precious subsection that with only one oscillator, the system is immediately chaotic. We will now study the usual trajectories that the central system will follow for only one oscillator. The conditions for the general parameters of these cases will be similar to the ones of the previous section.

FIGURA DE

TRAYECTORIA

TIPICA

In Figura (REFERENCIAR FIGURA ANTERIOR) we see a typical trajectory of the particle interacting with a harmonic oscillator, we see that the particle falls to one well and the other in an erratically way. The chaotic dynamics makes it difficult to predict to which side the particle will fall when the dynamics begins. The phase space trajectory permits the

FIGURA DE

TRAYECTORIA

OSCILADOR ARMONICO

ESPACIO DE FASE

In Figure (REFERENCIAR FIGURA ANTERIOR) we can see the phase space trajectory of the harmonic oscillator and how it is perturbed compared with a typical trajectory of a harmonic oscillator without a coupling whose orbits in phase space are perfect ellipses.

We can also see in Figure (REFERENCIAR FIGURA ANTERIOR) that the dynamics is antisymmetric with the inversion of the initial conditions of the harmonic oscillator $X_1 \rightarrow -X_1$ and $P_1 \rightarrow -P_1$.

3.2.4 Dynamics for 2 oscillators

When we start to increase the number of harmonic oscillators that compose the heat bath we start to evidence the tendency to stay on one well for a longer period of time as it is shown in Figure (REFERENCIAR FIGURA SIGUIENTE) .

FIGURA DE
TRAYECTORIA
TIPICA
DOS OSCI

The harmonic oscillators will share some of the initial energy of the particle for a longer time and this means that the particle will take longer to have again enough energy to jump from one well to the other.

3.3 Nature of the heat bath

It is natural to consider the possibilities in this particular problem were we can vary a big amount of parameters to search for different dynamics and properties that exhibit the system, the model is rich in quantities that can be calculated and extracted from it. This idea also plays against our odds because as there are many parameters to play with it is difficult to control the whole system in an optimal and hierarchical way. There are two types of parameters that we will monitor very closely: the frequency spectra and the energy spectra for the heat bath; these two parameters contain the information regarding the nature of the heat bath, meaning we can model different behaviors of the heat bath interacting with the particle. In this section we will give a little insight on the importance of correctly modeling the nature of the heat bath.

FIGURA
LAPIZ
BAÑO

The importance to model correctly the heat bath is related to the idea of this numerical experiment. We shall imagine this problem as a pencil perfectly balanced on its tip, it is of course an unstable equilibrium point, therefore the slightest perturbation of this pencil will cause the pencil to fall somewhere, if we imagine this on a two dimensional plane, the pencil

will either fall left or right. Then modeling the bath in a correct numerical way will give us the way these perturbations considered as an environment will affect the state of the initially balanced pencil. This environment may have different parameters to vary in order to have different dynamics for the pencil.

In principle we can consider the whole system of particle+bath as a compound closed system, but if we look at just the particle in the double well then it can be considered as an open system interacting with its environment given by the heat bath. When the number of oscillators in the heat bath is small, then the poincaré recurrence time will be also small as the particle will exchange energy with the heat bath in a short period of time. Nevertheless when the number of harmonic oscillators increases then the poincaré recurrence time will increase also, in the limit of infinite harmonic oscillators the poincaré recurrence time will also go to infinity producing dissipation phenomena in the system[8].

3.3.1 Frequency spectra

The way the frequencies of the harmonic oscillators are distributed in this work is taken from the theory of quantum dissipation in open systems. When the system is composed by a huge number of harmonic oscillators it is convenient to choose wisely how the frequencies of harmonic oscillators are distributed, therefore we may introduce the idea of the spectral density of bath modes as

$$J(\omega) = \pi \sum_{i=1}^{N} \frac{g_i^2}{2_i \omega_i} \delta(\omega - \omega_i). \tag{3.19}$$

This quantity will in fact give the information about how the heat bath's frequencies relate and include how the coupling to the system is chosen characterizing the bath. Depending on the system to be studied different values for the parameters may be taken to reproduce different dynamics, in the case of infinite modes this spectral density will relate to the damping integral kernel characterizing the Langevin dissipative dynamics.

In this work we will take the distribution of the frequencies as in standard open systems dynamics[13] [54][55]

$$J(\omega) \sim w^s f(\omega, \omega_c) \tag{3.20}$$

Where ω_c is the characteristic frequency of the bath, and $f(\omega, \omega_c)$ is a damping function which helps $J(\omega)$ to vanish in the limit of $\omega \to \infty$. There are many different ways to choose $f(\omega, \omega_c)$ [55], in this case we will choose an exponential cut-off damping type as $f(\omega, \omega_c) = e^{-\omega/\omega_c}$.

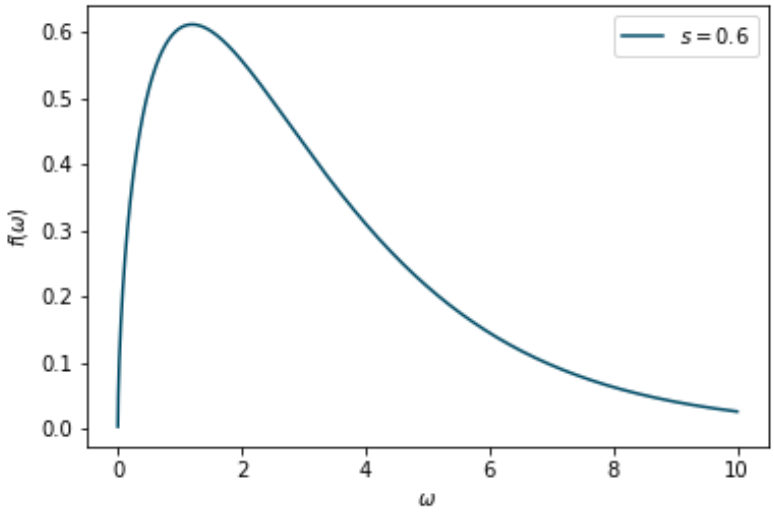

Figure 3.10: Frequency spectrum distribution without normalization for the case of $s = 0.6$.

3.3.2 Energy spectra

In this work we will monitor the energy spectra in two different ways, both are related to the idea of having a cloud of harmonic oscillators with initial conditions around the origin of phase space. The first idea is by drawing the energy of the oscillators from a distribution with a certain mean and variance, the second one consists of using the Box-Muller transform to sample a quasi-gaussian two dimensional distribution of harmonic oscillators in phase space. Essentially both of these cases will relate to a gaussian distribution in energies of the heat bath, we will model most of the times a cold heat bath i.e. with small energy compared to the central system, therefore it the energy distribution does not need to be necessarily a Boltzmann distribution.

3.3.2.1 Drawing energy from a distribution

The method outlined in this subsection consists on drawing the energy of each harmonic oscillator from a probability distribution (mostly a gaussian) with a determined mean and variance. This method will let us normalize the energy of the heat bath at will, having the energy of each harmonic oscillator will let us compute the sum and divide each energy by the normalization desired.

Now to decide where to locate each oscillator we sample a random number from a uniform distribution $[0, 2\pi)$, this will represent an angle on a circle which will be deformed into an ellipse according to the energy and frequency of each harmonic oscillator obtaining finally

a position of a harmonic oscillator according to a determined energy ellipse. This process is repeated for every oscillator on the bath giving as a result a distribution of oscillators in phase space with an energy distribution of the heat bath perfectly defined and normalized.

3.3.2.2 Quasi-gaussian distribution in phase space

This method consists in implementing the Box-Muller transform algorithm onto a uniform distribution to obtain a two dimensional distribution grid of points that represent a gaussian with a defined mean and variance along each dimension [56]. This method is important in the way that it allows us to have a gaussian distribution in phase space for the harmonic oscillators that can be canged at will to have a defined width along position or momentum as desired, this feedom in choosing the shape of the distribution gives us freedom in the nature of the heat bath on how the harmonic oscillators' motion changes in the initial conditions have different consequences in the particle's motion. This method can also be normalized efficiently.

3.4 Number of modes in the bath

A very important parameter to determine the dynamics of the system is the number of oscillators in the heat bath. According to dissipative dynamics theory, we retrieve an equation of Langevin type dynamics in the limit of infinite harmonic oscillators in the bath.We have already shown the behavior of the dynamics under the influence of only one harmonic oscillator coupled to the particle. What we will do in this work will be increase steadily the number of harmonic oscillators of a finite heat bath to achieve dissipative behavior without the need of extending the system to infinity. Therefore, it is important to keep an eye on the dynamics of each case of the number of harmonic oscillators and change different parameters of the system in order to understand in a more general way the behavior of the whole system as a function of the number of modes of the bath. This analysis will lead to the conclusion to modelate dissipative dynamics in a finite heath bath with a very small number of modes.

3.4.1 Chaos to dissipative dynamics

In this section we will start to evidence the loss of chaotic dynamics due to the increasing number of oscillators.

3.4.2 Variation of the double well and heat bath parameters

There are four types of parameters that are interesting for us to look at the variation of the dynamics of the system: The exponent s in the equation (3.20), the coupling constant of the oscillators g_0 that multiplies the coupling constant of each oscillator $g_i = g_0/\sqrt{N}$, the height of the potential barrier and the initial energy of the heat bath. Each of these conditions will affect the number of jumps from one well to the other that the particle makes. We will therefore evaluate the results of changing these parameters for different number of oscillators for 100 test cases where the positions, frequencies and energies are randomized every time and the numbers of jumps will be averaged. The way of sampling the energies and initial conditions are described in the method of drawing energies from a gaussian distribution in order to have more control on the energies of the harmonic oscillators. For most of the cases we will use fixed values for each parameter unless explicitly stated otherwise, these values are $s = 0.5$, $g_0 = 0.1$, the initial energy of the heat bath $E_{bath} = 0.1$ and the height of the potential barrier $PB = 1$

3.4.2.1 Changing the exponent s

According to the microscopic theory of dissipation [13], the exponent s in equation (3.20) controls the nature of the bath where $s = 1$ is the "ohmic" case where it can be compared to a dissipative term proportional to velocity in the classical equation. The case of $s > 1$ is called "super-ohmic" and the case of $0 < s < 1$ is called "sub-ohmic". Here we observe the behavior of the system in terms of the jumps between the wells seen for different numbers of harmonic oscillators and different values of the parameter s.

FIGURA FIGURE DE LOS SALTOS CAMBIANDO EL VALOR DE S

We conclude that for the classical case, the parameter s in the spectral density does not really affect the dynamics of the system in a particular way as we don't see a real difference between having a bath with sub-ohmic, ohmic or super-ohmic nature. We see the general behavior of dissipation where the jumps between the wells decrease with the increase in the in the number of oscillators in the heat bath and it is independent of the parameter s.

3.4.2.2 Changing the individual coupling g_0

We have seen the effect of the coupling involving chaos with only one oscillator in one of the previous sections, this showed us the effect of different values for the coupling constants that develop into increasing chaotic motion. In this section we will continue to study the effects on the dynamics of the whole system when we use different values for the constant g_0 that

multiplies each of the individual coupling constants $g_i \sim 1/\sqrt{N}$. Previously, the method we used to describe the dynamics and the effects of the change in the coupling was the Poincaré surface section, with this method we could visualize the increase of chaotic dynamics when the rational tori got destroyed. Unfortunately, when we increase the number of harmonic oscillators, the Poincaré sections stop being very useful, this is due to the amount of degrees of freedom the system will have. We could visualize the dynamics of the system because there was only two degrees of freedom, this made it possible to find planes where the dynamics was projected and this were the Poincaré surface sections, when we increase the number of oscillators the Poincaré planes will become hyperplanes that we cannot visualize properly, this means we would have to project the planes onto lower dimensions but doing this we would loose most of the details of the dynamics. For this reason we will visualize the change of the behavior using the same method of analysing the frequency of jumps between the wells.

We simulated the dynamics of the 100 test cases for different values of g_0 and different number of harmonic oscillators. We know from previous the experience of only one oscillator that if the coupling is strong the overall behavior will tend to be more chaotic, but now that we have more harmonic oscillators we start to see the effects of dissipation over chaos. A big coupling constant will continue to result in strong interactions between the oscillators and the particles, but the tendency of the particle to stay on one side will prevail.

FIGURA FIGURE DE LOS SALTOS CAMBIANDO EL VALOR DE G

In Figure (REFERENCIAR LA FIGURA ANTERIOR) we evidence that the overall tendency of dissipation is observed when the number of harmonic oscillators increases regardless the coupling constant g_0 (for $g = 0.001$ in the figure we believe for a bigger number of harmonic oscillators this behavior will be seen). It is also interesting to see that for coupling $g_0 = 0.3$ the curve descends really fast but seems to start to grow again, this can be attributed to the fact that this value for the coupling constant starts to be a very strong interaction of the bath with the system making it not very suitable for a dissipation model in long term.

3.4.2.3 Changing the initial energy of the heat bath

The initial energy of the heat bath is an important parameter statistically speaking, this is because it represents the "temperature" of the environment our central system is located in. If the whole system has initially a very high temperature then the dynamics will become very difficult to predict in long term as it will take longer time to reach a thermal equilibrium, if we take the temperature of the system to be relatively low compared to the height of the unstable equilibirum point where the particle is always located then we can see how energy from the particle is transfered to the heat bath in a somewhat irreversible manner.

This analysis involved then different initial energies for the heat bath and how it affects the number of jumps between the wells of the particle.

FIGURA FIGURE DE LOS SALTOS CAMBIANDO EL VALOR DE E_bath

In Figure (REFERENCIAR LA FIGURA QUE ACABO DE HACER) we can evidence that the different initial energies of the heat bath will result in a change of scale of the number of jumps that the particle suffers. The overall behavior of dissipation is continued to be present. For a heat bath with a high initial energy or "temperature" we see that the particle jumps between the wells more times than for a small energy but when the number of oscillators increases then the jumps decrease. When we "freeze" the heat bath by giving it a low initial energy we experience less jumps between the wells and a faster decay of it when the number of oscillators increase. Then we can conclude that the overall consequence of changing the initial energy of the heat bath will be a scaling factor in the exponential decay of the jumps.

3.4.2.4 Changing the height of the potential barrier

The particle of the central system is located on the unstable equilibrium unless otherwise stated for the simulations done in this work, then a very interesting parameter to study is the difference in the dynamics when the height of the potential barrier where the unstable equilibrium point is changed. We recall that the shape of the quartic potential for the particle is given by equation (3.9) where the parameters a and b are in charge of the shape of the double well potential. We have shown previously in equation (3.18) that the height of the potential barrier is completely determined by the parameters a and b and that the resonance frequency of small oscillations for the two minima is given by equation (3.13) which only depends on parameter a. This ideas are relevant to determine how to change the potential barrier height, in general there will be two ways in which we can change this height. If we change only b we will rescale the whole potential, this means that the resonance frequency will change and the particle will have to travel more distance in general to go from one well to the other. The difference between changing the height this way is shown in Figure (REF FIGURA VARIANDO SOLAMENTE B) where the shape of the potential is completely scaled.

PONER
FIGURA
FIGURE
VARIANDO
SOLO

B

The other way to change the height of the potential barrier is by changing both a and b but mantaining the ratio a/b, this ensures the roots of $V(x)$ to remain unchanged but makes the minimums of the potential deeper and as a consequence changing the height of the potential barrier as it is shown on Figure (REF FIGURA VARIANDO A Y B). It is to be noted that this change of the wells' dept will in fact change the frequency of small oscillations around the potential minima.

PONER

FIGURA

FIGURE

VARIANDO

A Y

B

The height of the potential barrier is an important parameter for the reason that whenever the particle is inside one of the wells it will need an energy near to the height of the potential barrier in order to be able to jump to the other side. If the potential barrier is small then the particle does not need a lot of energy to be given from the oscillators in order to be able to surpass it, while if the potential barrier is big then it will need the oscillators to synchronize in a way to be able to give the particle enough energy to jump to the other well. In Figure (REF FIGURA JUMPS VARIANDO LA PROFUNDIDAD) we test both cases of changing the height of the potential barrier. The results coincide with the intuition in the sense of more height means less jumps and less height means more jumps, also when the bath is composed of more harmonic oscillators then the number of jumps reduce significantly. In Figure (REF FIGURA JUMPS VARIANDO LA PROFUNDIDAD) we also evidence that there is not a significant difference on how we decide to change the height of the potential barrier as both cases have similar results on the counts of jumps.

CHAPTER 4

Approach to the Measurement theory

The measurement theory is right now a widely worked research branch of quantum physics and it is related to the intrinsic nature and foundations of quantum mechanics. In this chapter we will talk about how measurement is interpreted in classical mechanics and why it is difficult to find a somewhat correct interpretation of this phenomena in quantum physics. Finally we will talk about the result of this work and how it is related to this interesting subject.

4.1 Classical Measurement

The concept of classical measurement appears as a process in classical statistical mechanics. In this formalism the objects are not in phase space location but are represented by a probability distribution ρ as a state in space. This probability distribution can be evolved in time, this motion is governed by the Liouville equation given as

$$\frac{\partial \rho}{\partial t} = \{\rho, H\}, \tag{4.1}$$

this equation represents the probability distribution as an abstract fluid, with this in mind the probability flows along the hamiltonian trajectories of the system. From this equation the Liouville theorem can be derived, it states that the flow of the probability distribution is incompressible, hence the density of the vicinity of a given point traveling through phase space is constant in time and in a more general way the entropy of the system is conserved.

The probability distribution in classical mechanics is the closest analog we can find of the state vector in quantum mechanics, the way the Liouville equation (4.1) evolves the probability distribution in time is analogous to the Schrödinger equation given by

$$i\hbar\frac{d}{dt}\left|\Psi(t)\right\rangle = \hat{H}\left|\Psi(t)\right\rangle \tag{4.2}$$

in the quantum mechanical sense.

In the classical regime we can refer to classical statistical measurement process. This states that you, as an observer, can learn something about the phase space determined of the system. In this framework, the process is to use your knowledge to reduce the probability distribution of the classical state of the system to a smaller volume, thus reducing the entropy of the system. This second process is totally related to the observation procedure and is not directly related to the equations of motion of the system, it is moreover involved with the abstract concept of the probability distribution we use.

We will now introduce the notions of classical information theory which can be applied to both continuous and discrete variables, to make things easier we will focus on the case of continuous variables. Let us consider shannon entropy bla blah

4.2 Quantum Measurement

The standard textbook approach to quantum mechanics considers this theory to be an inherently probabilistic theory [57][58][45], this means that quantum mechanics can make predictions about the results of measurements but most of the times just in a probabilistic way. The few cases where measurements have deterministic outcomes happens when the system is in an eigenstate of an observable and this observable is the one that will be measured. In most of the cases, even if we have full knowledge about the quantum mechanical state of the system and its characteristics, the outcome of measurements remain in principle as a random process. We can provide a simple illustration of this idea by considering a system with n states, the space of states will be held by the states $\left|1\right\rangle, \left|2\right\rangle, ..., \left|n\right\rangle$. We suppose that we know that the system is initially in the superposition state $psi = \sum_{i=1}^{n} \chi_i \left|i\right\rangle$, where χ_i are complex probability amplitudes and the completeness relation follows as $psi = \sum_{i=1}^{n} \left|\chi_i\right|^2$, and the question here will be to test if we find the system in the state $\left|j\right\rangle$. We can test our hypothesis by considering the operator for the observable $\hat{O}$ as a projector operator $\hat{O} = \left|j\right\rangle\left\langle j\right|$, this is a very illustrative example because it projects the system onto the state $\left|j\right\rangle$. When the operator is applied to the initial state we obtain the result of the measurement to be one (the system to be in the state $\left|j\right\rangle$) with probability $\left|\chi_j\right|^2$ and zero (the system is in any other

state) with probability $1 - |\chi_j|^2$.

This is the general scheme of a quantum measurement in the context of orthodox quantum mechanics, recently there have been some attempts to evaluate different ways to explain the process of quantum measurement that try to explain what happens during the process the measurement of the abstract state and returns a real measurement.

4.2.1 Postulates of Quantum Mechanics

The way we understand quantum mechanics is related to its mathematical formulation and structure, this mathematical formulation relies in the theory of abstract algebra and in particular mostly on the theory of Hilbert spaces. This formulation leads to what we call the postulates of quantum mechanics, which is the handbook for the rules of quantum mechanics. We will not talk about all the postulates but we will emphasize on the ones that illustrate the measurement and the order will follow Cohen-Tannoudji's order [57].

- Second Postulate: Every measurable physical quantity Q is described by an operator $\hat{Q}$; this operator is called an observable.
- Third Postulate: The only posible result of the measurement of a physical quantity Q is one of the eigenvalues of the corrensponding observable $\hat{Q}$.
- Fourth Postulate: When a measurement of an observable $\hat{Q}$ is made on a generic state $|\psi\rangle$, the probability of obtaining an eigenvalue q_n is given by the square of the inner product of the state $|\psi\rangle$ with the eigenstate $|q_n\rangle$, $|\langle q_n|\,|\psi\rangle|^2$.
- Fifth Postulate (collapse): If the measurement of the physical quantity Q on the system in the state $|\psi\rangle$ gives the result q_n, the state of the system immediately after the measurement is the normalized eigenstate $|q_n\rangle$ (this is of course the postulate most difficult to digest as it involves what we call the collapse of the superposition state of the wave function into just one measurable state).

4.3 Can our model be considered as a measurement?

The short answer to this question would be yes, as we previously compared this system to a quantum system with continuous variables. One of the postulates of quantum mechanics is about the collapse of the wave function into one of the eigenstates of the system, this means that every time we measure the system again we would in fact have probability one to obtain the system on the same eigenstate, this means the state measured is stationary over time.

We can consider our system to follow this argument: when the system is evolved in time, the particle initially in a neutral state on top of the energy barrier will fall into one of the wells, as we concluded in the previous sections, when we increase the number of modes in the bath the particle will dissipate its energy and remain on one of the wells for longer time in an asymptotic way resembling a measurement. Therefore every time we check the system again we will find the particle on the same well as the previous measurements as if it was the eigenstate that the system collapsed into.

CHAPTER 5

Related work

This whole project is a small part of a bigger picture considering the same ideas but related to quantum measurement. This classical analogue of the spin measurement is not a direct classical version of it but it is the closest analogue we might find.

5.1 Quantum measurement in a unitary setting

The goal of this project is to treat quantum measurement in the standard unitary setting as a process that might not involve randomness in its outcome.

chapter 6

Conclusion

Bibliography

[1] Maximilian Schlosshauer. Decoherence, the measurement problem, and interpretations of quantum mechanics. *Reviews of Modern physics*, 76(4):1267, 2005.

[2] R Brown and DJ Mazey. The philosophical magazine. *or Annals of Chemistry, Mathematics, Astronomy, Natural History and General Science*, 4:161–173, 1828.

[3] Albert Einstein et al. On the motion of small particles suspended in liquids at rest required by the molecular-kinetic theory of heat. *Annalen der physik*, 17(549-560):208, 1905.

[4] Ryogo Kubo. Brownian motion and nonequilibrium statistical mechanics. *Science*, 233(4761):330–334, 1986.

[5] Paul Langevin. Sur la théorie du mouvement brownien. *Compt. Rendus*, 146:530–533, 1908.

[6] VV Flambaum and FM Izrailev. Statistical theory of finite fermi systems based on the structure of chaotic eigenstates. *Physical Review E*, 56(5):5144, 1997.

[7] VV Flambaum and FM Izrailev. Distribution of occupation numbers in finite fermi systemsand role of interaction in chaos and thermalization. *Physical Review E*, 55(1):R13, 1997.

[8] Peter Mazur and Elliott Montroll. Poincaré cycles, ergodicity, and irreversibility in assemblies of coupled harmonic oscillators. *Journal of mathematical physics*, 1(1):70–84, 1960.

[9] GW Ford and RF O'Connell. Radiating electron: Fluctuations without dissipation in the equation of motion. *Physical Review A*, 57(4):3112, 1998.

[10] S Taylor Smith and Roberto Onofrio. Thermalization in open classical systems with finite heat baths. *The European Physical Journal B*, 61(3):271–275, 2008.

[11] Hideo Hasegawa. Classical small systems coupled to finite baths. *Physical Review E*, 83(2):021104, 2011.

[12] AO Caldeira and Anthony J Leggett. Quantum tunnelling in a dissipative system. *Annals of physics*, 149(2):374–456, 1983.

[13] Anthony J Leggett, SDAFMGA Chakravarty, Alan T Dorsey, Matthew PA Fisher, Anupam Garg, and Wilhelm Zwerger. Dynamics of the dissipative two-state system. *Reviews of Modern Physics*, 59(1):1, 1987.

[14] Edward Ott. *Chaos in dynamical systems*. Cambridge University Press, Cambridge, U.K. ; New York, 2nd ed edition, 2002.

[15] Jesus-Maria Sanz-Serna and Mari-Paz Calvo. *Numerical hamiltonian problems*. Courier Dover Publications, 2018.

[16] Herbert Goldstein, Charles Poole, and John Safko. Classical mechanics, 2002.

[17] VI Arnold and A Avez. Probemes ergodiques de la mécanique classique, gauthier-villars, 1967; ergodic problems of classical mechanics, 1968.

[18] George M Zaslavsky and Georgij Moiseevič Zaslavskij. *Hamiltonian chaos and fractional dynamics*. Oxford University Press on Demand, 2005.

[19] George M Zaslavsky. *The physics of chaos in Hamiltonian systems*. world scientific, 2007.

[20] João Carlos Xavier. Banhos caóticos finitos: relação entre dissipação e expoentes de lyapunov. 2015.

[21] Allan J Lichtenberg and Michael A Lieberman. *Regular and chaotic dynamics*, volume 38. Springer Science & Business Media, 2013.

[22] George Contopoulos. *Order and chaos in dynamical astronomy*. Springer Science & Business Media, 2004.

[23] Loup Verlet. Computer" experiments" on classical fluids. i. thermodynamical properties of lennard-jones molecules. *Physical review*, 159(1):98, 1967.

[24] Etienne Forest and Ronald D Ruth. Fourth-order symplectic integration. *Physica D: Nonlinear Phenomena*, 43(1):105–117, 1990.

[25] Ronald D Ruth. A canonical integration technique. *IEEE Trans. Nucl. Sci.*, 30(CERN-LEP-TH-83-14):2669–2671, 1983.

[26] Paul J Channell. Symplectic integration algorithms. *Preprint, Los Alamos National Laboratory, Los Alamos, NM, USA*, 1983.

[27] Curtis R Menyuk. Some properties of the discrete hamiltonian method. *Physica D: Nonlinear Phenomena*, 11(1-2):109–129, 1984.

[28] Kang Feng and Mengzhao Qin. *Symplectic geometric algorithms for Hamiltonian systems*. Springer, 2010.

[29] Feng Kang and Wang Dao-liu. Symplectic difference schemes for hamiltonian systems in general symplectic structure. *Journal of Computational Mathematics*, pages 86–96, 1991.

[30] Paul J Channell and Clint Scovel. Symplectic integration of hamiltonian systems. *Nonlinearity*, 3(2):231, 1990.

[31] D Markiewicz. Survey on symplectic integrators. *Preprint Univ. California at Berkeley, Spring*, 1999.

[32] Rene De Vogelaere. Methods of integration which preserve the contact transformation property of the hamilton equations. *Technical report (University of Notre Dame. Dept. of Mathematics)*, 1956.

[33] René Lozi. Can we trust in numerical computations of chaotic solutions of dynamical systems? In *Topology and dynamics of Chaos: In celebration of Robert Gilmore's 70th birthday*, pages 63–98. World Scientific, 2013.

[34] Zbigniew Galias. Are numerical studies of long term dynamics conclusive: the case of the hénon map. In *Journal of Physics: Conference Series*, volume 692, page 012001. IOP Publishing, 2016.

[35] Vladimir I Arnold. Proof of a theorem of an kolmogorov on the invariance of quasi-periodic motions under small perturbations of the hamiltonian. *Collected Works: Representations of Functions, Celestial Mechanics and KAM Theory, 1957–1965*, pages 267–294, 2009.

[36] Andrey Nikolaevich Kolmogorov. On conservation of conditionally periodic motions for a small change in hamilton's function. In *Dokl. Akad. Nauk SSSR*, volume 98, pages 527–530, 1954.

[37] Michael Tabor. *Chaos and integrability in nonlinear dynamics: an introduction*. Wiley, 1989.

[38] Persi Diaconis, Susan Holmes, and Richard Montgomery. Dynamical bias in the coin toss. *SIAM review*, 49(2):211–235, 2007.

[39] Pu Li, Yun-Cai Wang, and Jian-Zhong Zhang. All-optical fast random number generator. *Optics express*, 18(19):20360–20369, 2010.

[40] Pu Li, Yuanyuan Sun, Xianglian Liu, Xiaogang Yi, Jianguo Zhang, Xiaomin Guo, Yanqiang Guo, and Yuncai Wang. Fully photonics-based physical random bit generator. *Optics letters*, 41(14):3347–3350, 2016.

[41] Anbang Wang, Pu Li, Jianguo Zhang, Jianzhong Zhang, Lei Li, and Yuncai Wang. 4.5 gbps high-speed real-time physical random bit generator. *Optics express*, 21(17):20452–20462, 2013.

[42] Michael Ghil and Stephen Childress. *Topics in geophysical fluid dynamics: atmospheric dynamics, dynamo theory, and climate dynamics*, volume 60. Springer Science & Business Media, 2012.

[43] X Liu and Z Zhai. Location identification for indoor instantaneous point contaminant source by probability-based inverse computational fluid dynamics modeling. *Indoor air*, 18(1):2–11, 2008.

[44] Max Born. Statistical interpretation of quantum mechanics. *Science*, 122(3172):675–679, 1955.

[45] John Archibald Wheeler and Wojciech Hubert Zurek. *Quantum theory and measurement*. Princeton University Press, 2014.

[46] Wojciech Hubert Zurek. Decoherence, einselection, and the quantum origins of the classical. *Reviews of modern physics*, 75(3):715, 2003.

[47] Wojciech Hubert Zurek. Quantum darwinism. *Nature physics*, 5(3):181–188, 2009.

[48] Walther Gerlach and Otto Stern. Der experimentelle nachweis der richtungsquantelung im magnetfeld. *Zeitschrift für Physik*, 9(1):349–352, 1922.

[49] Thomas Dittrich. Quantum chaos and quantum randomness—paradigms of entropy production on the smallest scales. *Entropy*, 21(3):286, 2019.

[50] Amir O Caldeira and Anthony J Leggett. Influence of dissipation on quantum tunneling in macroscopic systems. *Physical Review Letters*, 46(4):211, 1981.

[51] Stephen K Gray, Donald W Noid, and Bobby G Sumpter. Symplectic integrators for large scale molecular dynamics simulations: A comparison of several explicit methods. *The Journal of chemical physics*, 101(5):4062–4072, 1994.

[52] Jesús Maria Sanz-Serna and Mari-Paz Calvo. Symplectic numerical methods for hamiltonian problems. *International Journal of Modern Physics C*, 4(02):385–392, 1993.

[53] Christopher Rackauckas and Qing Nie. Differentialequations. jl–a performant and feature-rich ecosystem for solving differential equations in julia. *Journal of Open Research Software*, 5(1), 2017.

[54] Haobin Wang and Michael Thoss. From coherent motion to localization: Ii. dynamics of the spin-boson model with sub-ohmic spectral density at zero temperature. *Chemical Physics*, 370(1-3):78–86, 2010.

[55] Haobin Wang and Michael Thoss. From coherent motion to localization: dynamics of the spin-boson model at zero temperature. *New Journal of Physics*, 10(11):115005, 2008.

[56] George EP Box. A note on the generation of random normal deviates. *Ann. Math. Stat.*, 29:610–611, 1958.

[57] C Cohen-Tannoudji, B Diu, and F Laloe. Quantum mechanics vol. 1.[sl], 1978.

[58] Albert Messiah. *Quantum mechanics*, volume 2. Elsevier, 1981.

appendix A

Extra Information

Some more text ...